NASA TECHNICAL NOTE

NASA TN D-5020

SCIENTIFIC EXPERIMENTS FOR THE APOLLO TELESCOPE MOUNT

George C. Marshall Space Flight Center
Huntsville, Ala.

NATIONAL AERONAUTICS AND SPACE ADMINISTRATION • WASHINGTON, D. C. • MARCH 1969

SCIENTIFIC EXPERIMENTS FOR THE APOLLO TELESCOPE MOUNT

George C. Marshall Space Flight Center
Huntsville, Ala.

NATIONAL AERONAUTICS AND SPACE ADMINISTRATION

For sale by the Clearinghouse for Federal Scientific and Technical Information
Springfield, Virginia 22151 – CFSTI price $3.00

PREFACE

In 1966, at the time the Apollo Telescope Mount Project was assigned to the Marshall Space Flight Center, the Space Sciences Laboratory was requested to provide a Project Scientist for the overall project, and an Experiment Scientist for each of the five experiments. The role of the Experiment Scientists was defined as follows: "to interface with the scientific community, to assure the scientific integrity of the experiments, and to assure that scientific objectives are met."

The Space Sciences Laboratory, having been interested in the Apollo Telescope Mount even prior to its assignment to MSFC, has enjoyed a close relationship with the primary research and design organizations during the development of the ATM. In addition to providing scientific support, the Space Sciences Laboratory has contributed in areas such as: radiation effects and the problem of film fogging, optical contamination and its effects on the experiments, and the evaluation of the contaminating effects of thermal vacuum test chambers.

This report is a compilation of data and experiment descriptions prepared by the Experiment Scientists, complemented by information obtained during a close association with the experiments and the Principal Investigators.

Ernst Stuhlinger

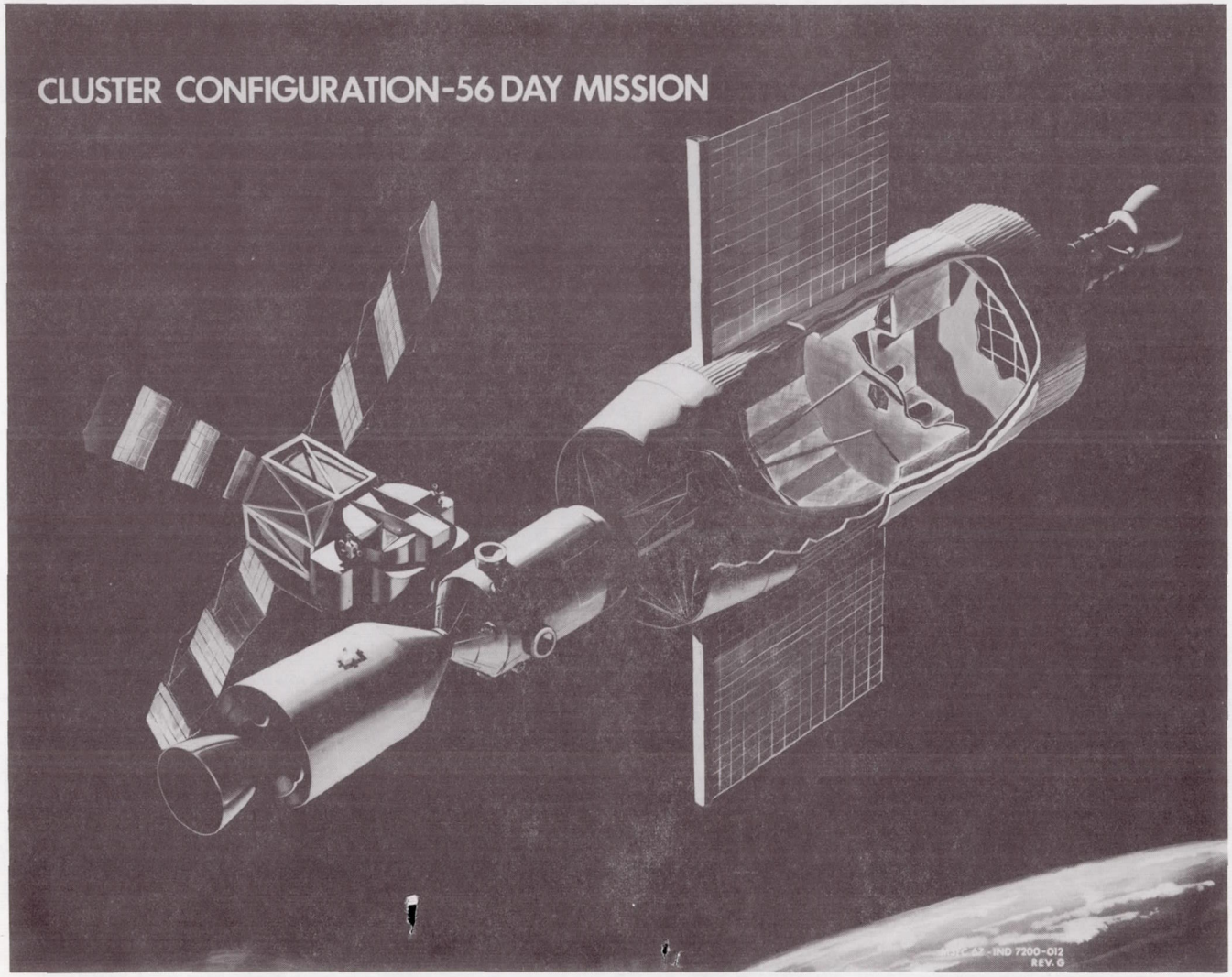

FRONTISPIECE

TABLE OF CONTENTS

LIST OF ILLUSTRATIONS

LIST OF ILLUSTRATIONS (Concluded)

LIST OF TABLES

SCIENTIFIC EXPERIMENTS FOR THE APOLLO TELESCOPE MOUNT

SUMMARY

The Apollo Telescope Mount is to be a manned solar observatory to make measurements of the sun by placing telescopes and instruments above the earth's atmosphere. These instruments will obtain data on the transitions occurring in elements ionized in the vicinity of the sun's surface. These data are contained in the ultraviolet and x-ray spectrum that is almost completely absorbed by the earth's atmosphere. Orbiting telescopes would also observe flares and regions of the corona that are either hidden to telescopes on earth or are covered with scattered light. The white light coronagraph experiment (High Altitude Observatory experiment) will therefore be operated outside the light scattering effects of the earth's atmosphere. Two ultraviolet experiments (Harvard College Observatory and Naval Research Laboratory experiments) will obtain spectral line intensity and high spectral resolution measurements. Two x-ray experiments (American Science and Engineering and Goddard Space Flight Center experiments) will be used to study solar flares and the dynamics of the solar atmosphere. Descriptions of these five experiments and the associated equipment are presented in this report.

INTRODUCTION

By

James Dozier
and Edwin Klingman

The mysteries of the nature and the origin of the heavenly bodies have fascinated man for the length of his existence. Attempts to gain insight into these mysteries have led man to attempt to overcome the natural limitations to which his observations are subject. Earlier limitations were almost entirely instrumental in nature. The invention, development, and improvement of the optical telescope, the radio receiver, and electronic and photographic detectors in all spectral regions have now progressed to the point where ground-based astronomical observations are essentially free of instrumental limitations. Information theory and automatic data processing have even provided the means for optimizing the information content from a fixed amount of data. There still exists a limitation on ground-based astronomy that no amount of technological advancement will overcome: the atmosphere. Only by placing suitable telescopes above the atmosphere will several severe problems be solved.

The most severe problem caused by the atmosphere is opacity in certain wavelength regions. Figure 1 illustrates the opacity as a function of wavelength and the wavelength regions of interest to the Apollo Telescope Mount (ATM) project. A large part of the infrared spectrum and all of the ultraviolet and x-ray spectrum are almost totally absorbed in the atmosphere. There are valid reasons why this portion of the spectrum is of interest to science. Certain regions of the sun exist at temperatures high enough to cause partial ionization of all elements present. From these regions the only transitions occurring are in the extreme ultraviolet and x-ray regions. To obtain data on such transitions that will give information about stellar processes and heating mechanisms is one of the major goals of the ATM project. The sole concern is not merely with the existence of those transition lines. The pointing capability of a manned high resolution orbiting telescope will allow the determination of temperature changes across boundaries of supergranulation. Spatial scans at the limb of the sun would allow determination of the difference in apparent size of the sun from line to line, thus yielding information on the distribution of ions in the corona. This information would be invaluable in calculating the temperature and density structure of the low corona. Pointing capabilities combined with on-the-spot

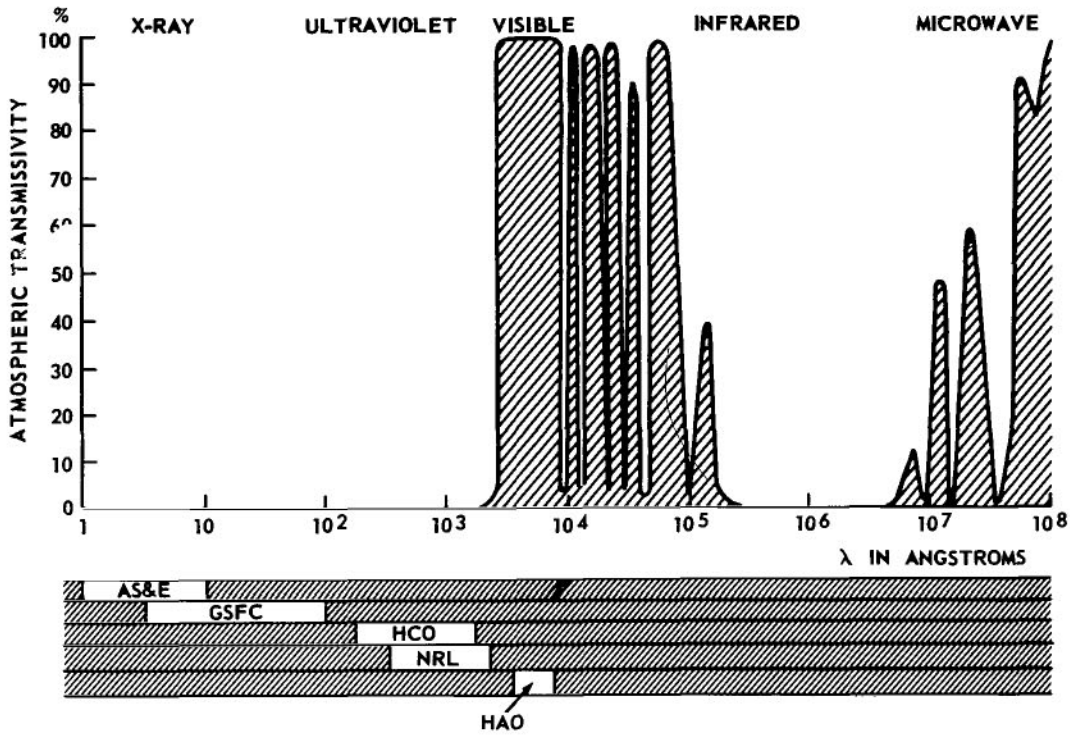

FIGURE 1. REGIONS OF SPECTRUM OF INTEREST TO ATM INCLUDING ATMOSPHERIC TRANSMISSIVITY AS A FUNCTION OF WAVELENGTH

decisions possible with a manned telescope will allow the study of flares, particularly in the early phases of their development. The ultraviolet measurements will be made by the Harvard College Observatory and the Naval Research Laboratory (NRL) instruments. Information from the x-ray region will be measured by the Goddard and the American Science and Engineering x-ray telescopes.

The two ultraviolet experiments measure overlapping portions of the spectrum. The reason for this is simple. The Harvard experiment uses electronic detectors which yield precise intensity measurements but only moderate spectral resolution. The NRL experiment, on the other hand, uses photographic detection systems which provide extremely high spectral resolution with only moderate intensity measurements. The two combine to maximize the obtainable information from this region of the spectrum. In a similar manner, the x-ray experiments complement each other.

There is still another atmospheric problem that affects even those regions of the spectrum which are not absorbed in the atmosphere. This is the scattering of light from scattering centers in the atmosphere. The result of such scattering is to cover low intensity sources with a background of "noise" or scattered light. This is the reason that stars are not visible in daylight. Another result of scattering is the impossibility of obtaining complete measurements of the solar corona. The regions of the corona which are farthest from the sun are completely hidden to ground-based telescopes. The High Altitude Observatory white light coronagraph is designed to take advantage of the lack of scattering above the atmosphere.

It should also be noted that for a long time observing instruments were diffraction-limited. Now the state of the art is such that for instruments larger than 30.5 cm (12 in.), it is useless to build diffraction-limited telescopes.* The diffraction or scintillation caused by thermal motion in the air with resultant changes of indices of refraction is greater than instrumental diffraction. This effect is seen in the twinkling of stars.

To overcome any or all of the above limitations inherent in ground-based observations, it is necessary to use a telescope above the atmosphere. If such a telescope is to be used to obtain maximum information, it must be manned. The ATM program is designed to achieve this goal.

ATM SUPPORT BY SPACE SCIENCES LABORATORY PERSONNEL

ATM Project Scientist: Dr. J. Dozier, R-SSL-P, 876-5179

ATM Asst. Project Scientist: Dr. A. deLoach, R-SSL-P, 876-5179

ATM Project Officer: H. Dudley, R-SSL-X, 876-1617

Experiment Scientists:

S 052
J. McGuire, R-SSL-S, 876-7571

*Although conversions to Standard International Units were made in the text of this report, the engineering data in the figures and Appendices are primarily in English units.

S 082A/S 082B
G. Arnett, R-SSL-T, 876-3314

S 054
S. Fields, R-SSL-T, 876-0582

S 055A
E. Klingman, R-SSL-P, 876-1865

S 056
Dr. A. deLoach, R-SSL-P, 876-5179

MSFC H-α #2 Experiment Scientist: E. Miller, R-SSL-T, 876-4861

ATM Optical Contamination Investigation Project Scientist: Dr. J. Dozier, R-SSL-P, 876-5179

ATM Optical Contamination Flight Experiment Project Engineer: L. Yarbrough, R-SSL-S, 876-4619

ATM Thermal Vacuum Testing Representative: J. Zwiener, R-SSL-T, 876-4861

ATM Related Solar Telescope Project Scientist: E. Wells, R-SSL-S, 876-7571

ATM Thermal Design Representative: G. Heller, R-SSL-T, 876-4024

ATM Radiation Effects Investigation Project Scientist: Dr. A. deLoach, R-SSL-P, 876-5179

Proton Spectrometer Project Physicist: L. Breazeale, R-SSL-N, 876-3444

Real-Time Solar Magnetograph Project Manager: W. Snoddy, R-SSL-T, 876-8701

Table I gives a breakdown of the ATM experiments that are discussed in this report.

TABLE I. ATM EXPERIMENTS

Number	Title	Organization	Contacts*		Purpose
S 052	White Light Coronagraph	High Altitude Observatory	PI ES Alt. ES EE	G. Newkirk J. McGuire R. Harwell	Measure brightness, form, and polarization of corona from 1.5 to 6 solar radii and correlate with sunspot and flare activity.
S 082A/ S 082B	UV Coronal Spectrographs	Naval Research Laboratory	PI ES Alt. ES EE	J. Purcell G. Arnett G. Heller J. Franks	Obtain high resolution pictures of short time variations in the solar atmosphere.
S 054	X-Ray Spectrographic Telescope	American Science & Engineering	PI ES Alt. ES EE	R. Giacconi S. Fields John Reynolds T. Ponder	Study flares in soft x-rays (2 to 8 Å) with high spectral and spatial resolution to understand flare mechanism.
S 055A	UV Spectrometers	Harvard College Observatory	PI ES Alt. ES EE	L. Goldberg E. Klingman J. Dozier J. Power	Monitor discrete ultraviolet lines to study the mechanisms of activity in the photosphere and chromosphere.
S 056	X-Ray Telescope	Goddard Space Flight Center	PI ES Alt. ES EE	J. Milligan A. deLoach R. Shelton H. Burke	Measure the intensity of solar flares with spatial and temporal resolution to understand the dynamics of the solar atmosphere.

*PI = Principal Investigator
ES = Experiment Scientist
Alt. ES = Alternate Experiment Scientist
EE = Experiment Engineer

WHITE LIGHT CORONAGRAPH (S 052, HIGH ALTITUDE OBSERVATORY)

By

Jim McGuire

Advances in our knowledge of the solar corona have primarily been brought about by advances in observing techniques. The fruitful studies of the corona in x-ray and radio wavelengths loom as outstanding examples of this premise. These developments, coupled with the perfection of the coronagraph by Lyot in 1930, are responsible for nearly all of our knowledge about the structure of the inner corona. These techniques, productive as they have been, have the serious drawback of revealing only the structure of the innermost corona. Many of the most exciting unsolved problems of coronal physics are thus to be found in the intermediate and outer corona ($2R < R < 6R$). Here coronal streamers take on their unique identity and the coronal gas is accelerated to become the solar wind. A few of these problems are suggested below.

1. What is the three-dimensional structure of coronal streamers?

2. Are they cylindrical forms or are they fanlike structures with considerable extent in longitude?

3. What connection exists between coronal streamers and such surface features as plages and magnetic regions?

4. How does the temporal development of coronal structures follow that of the associated surface features?

5. How does the solar wind vary from location to location in the corona?

6. How does the solar wind interact with the surface magnetic fields to form the coronal structures which we observe?

7. Which of the several proposed mechanisms for Type II, Type III, and Type IV radio bursts are dominant in producing the observed events?

8. Do radio bursts produce an optical counterpart?

Although it would be presumptuous to claim that continuous optical observation of the K corona will allow solution of all of these problems, it appears safe to say that they cannot be solved without the continuous optical observations.

A brief examination of the requirements which these problems place on the observations is in order. Clearly, the questions relating to the three-dimensional structure of coronal forms and their connection with surface features require at least daily photometric observation for a good fraction of solar rotation. The evolution of coronal structures and their connection with the interplanetary medium require similar observations extending over several solar rotations. Direct observations of the solar wind sweeping coronal inhomogeneities into space are probably not to be hoped for; but the combination of synoptic observations of the intermediate corona and radar measurements may well yield a more definitive estimate of solar wind velocities near the sun than the radar measures alone can supply. Again, corroborative observation of radio bursts at both optical and radio wavelengths may allow us to establish the number of electrons which are taking part in the event, to choose the appropriate excitation mechanism for the radio disturbance, and to establish the efficiency of the process. The remote possibility that a fraction of the optical radiation is due to the synchrotron mechanism can be explored by making complete polarization measurements.

The ATM coronagraph is eminently suited for these investigations and should be able to make valuable contributions in the above problem areas, except, perhaps, that of the long term evolution of coronal structures.

Table II lists various known solar disturbances with their characteristic velocities, and the time, t, for the disturbances to travel 1R. The period Δt is the time in which the disturbance travels a distance equal to the 15 arc sec resolution of the ATM White Light Coronagraph Experiment.

TABLE II. SOLAR DISTURBANCE CHARACTERISTICS

Disturbance	v(km/sec)	t	Δt
Type III Radio Bursts	0.9×10^5	7 sec	0.1 sec
Type II Radio Bursts or Solar Wind	10^3	11.6 min	10 sec
Coronal Whip	10^2	116 min	1.5 sec
Coronal Motions in "Helmets"	10	19.3 hr	16 min

Only in the case of the fast Type III bursts would observations be limited by instrumental resolution.

Since part of the justification for the ATM coronagraph is the hope of observing the passage of a flare-induced disturbance through the intermediate corona, we have calculated the probability of observing such an event during the mission. For this purpose we have used the flare data given by Smith and Smith (1963) for the year 1948 as representative of the conditions expected in the similar, near-maximum years 1969-1970 of the Apollo Applications Program mission. For 1948 the corrected flare incidence for flares of importance 1 or greater was 0.10 per hour for the visible hemisphere.

Since disturbance of the visible corona might be expected by flares within the longitude zones 30 deg on either side of the limb, we reduce the flare frequency to 0.06 per hour. The anticipated observing time of 3 hours per day for a 56-day mission will allow a total of 168 hours of operation of the ATM. Assuming that a fourth of the observing time could be devoted to the coronagraph, we find that the total coronal observing time is 42 hours. Thus, by blind chance in randomly selected observing intervals, we should expect to catch 2 - 3 limb flare events. Selection of the observing intervals for particularly auspicious times would increase the number of observed limb events considerably.

There has been an increased interest in the possibility of interplanetary material collecting at the equilateral, lunar Lagrange points L_4 and L_5. Thus far, nighttime photometry of these locations has led to rather equivocal answers about whether such a concentration exists. We hope to settle the issue with the ATM coronagraph. If observations can be made during the time that either of the points is passing near the sun, their presence should become apparent because of the preferential forward scattering that is to be expected from the interplanetary particles.

Description of the Instrument

The S 052 instrument is an externally occulted coronagraph (Fig. 2). This instrument is designed to block out the image of the sun's disk and to take white light pictures of the sun's corona. The optics and electronics are contained in a 0.685 m (27-in.) long sealed housing at the rear of the instrument (Fig. 3). Three external occulting disks are mounted 2.11 m (83 in.) forward of the optics housing. Both the occulting disk assembly and the optics housing are mounted to an optical bench which then mounts to the ATM rack. The space between the front of the optics housing and the external occulting disks is enclosed in a light baffle tube, and the experiment camera mounts on the rear of the optics housing.

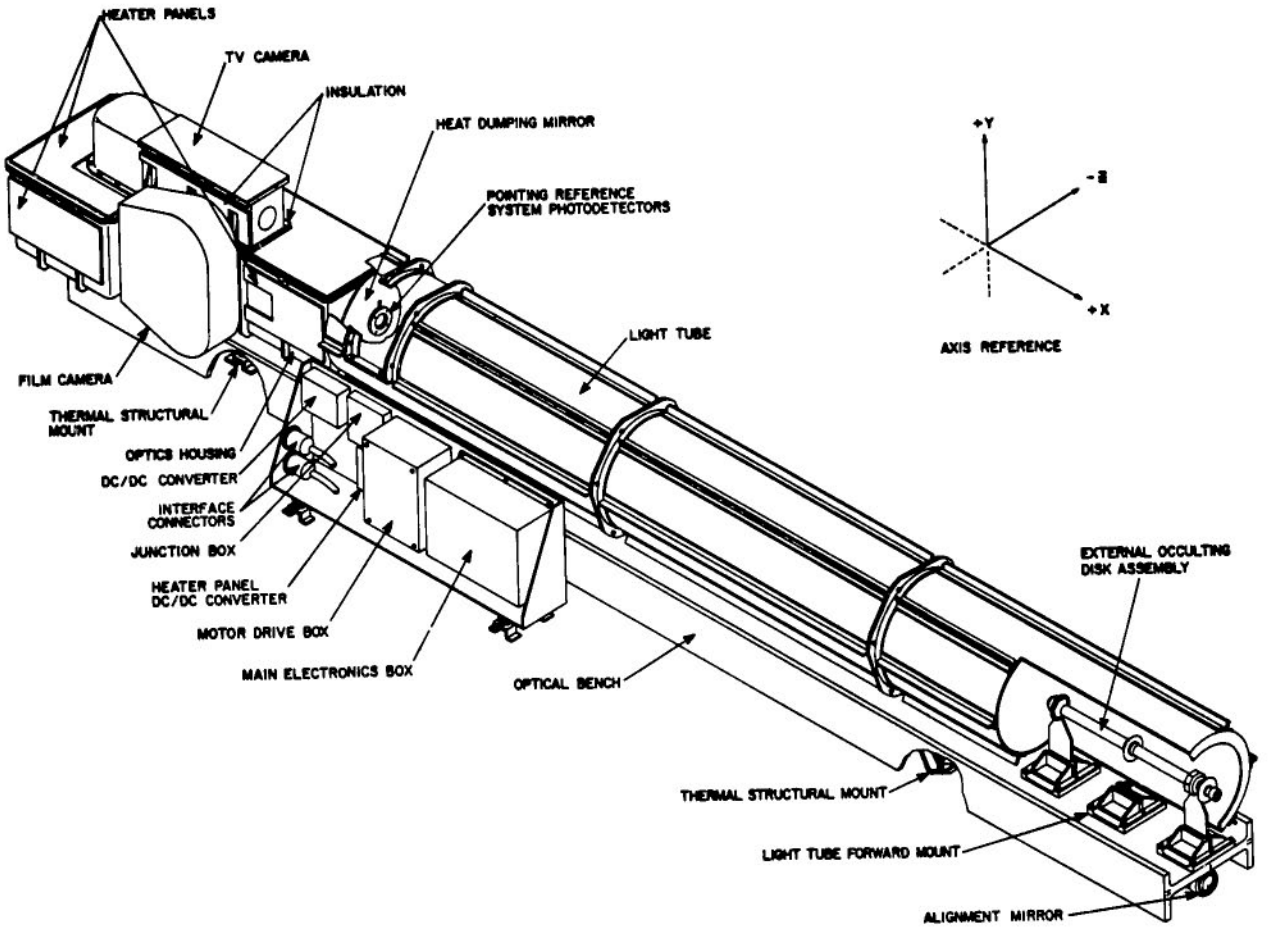

FIGURE 2. SCHEMATIC OF THE EXTERNALLY OCCULTED CORONAGRAPH

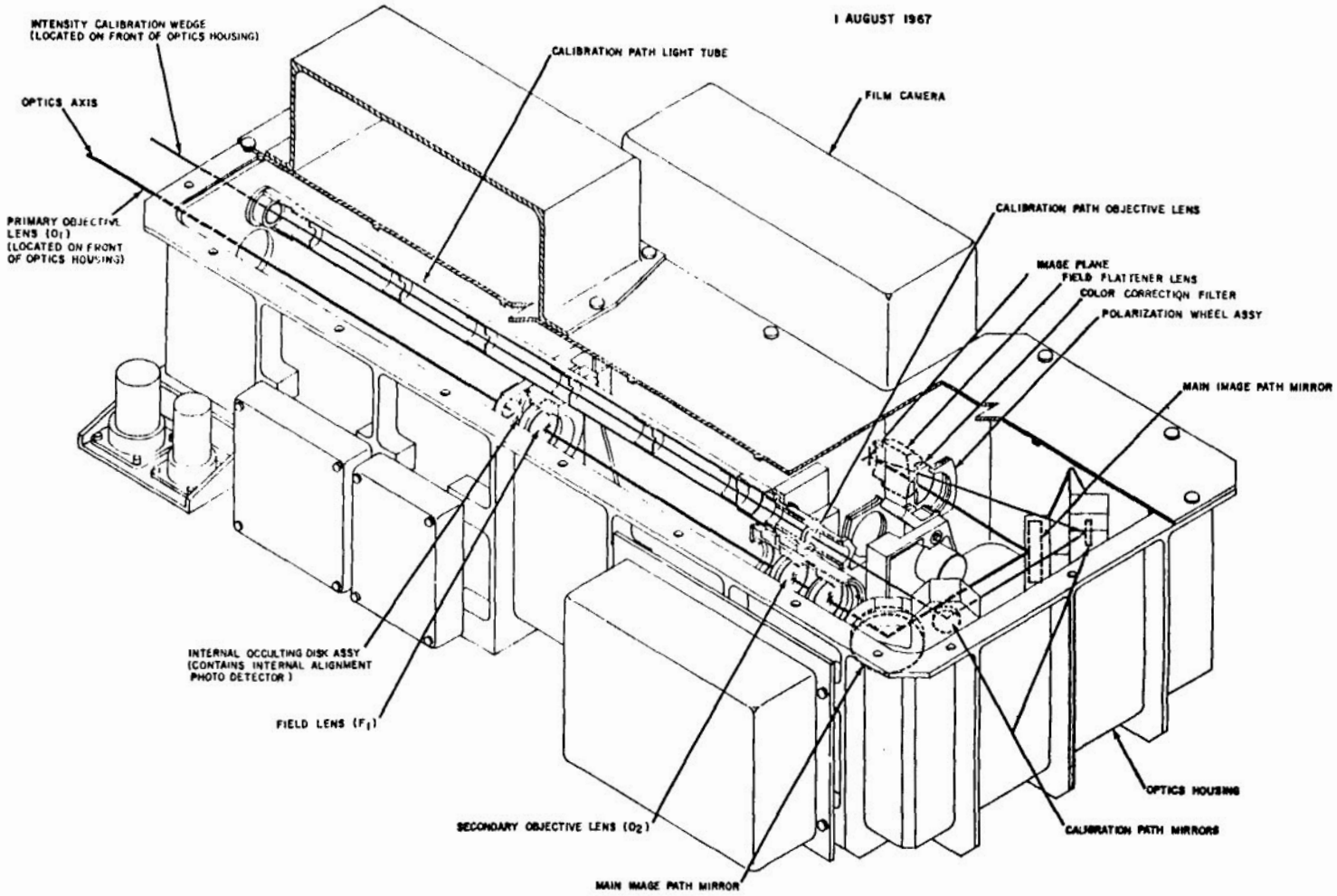

FIGURE 3. OPTICAL AND ELECTRONIC COMPONENTS IN SEALED HOUSING

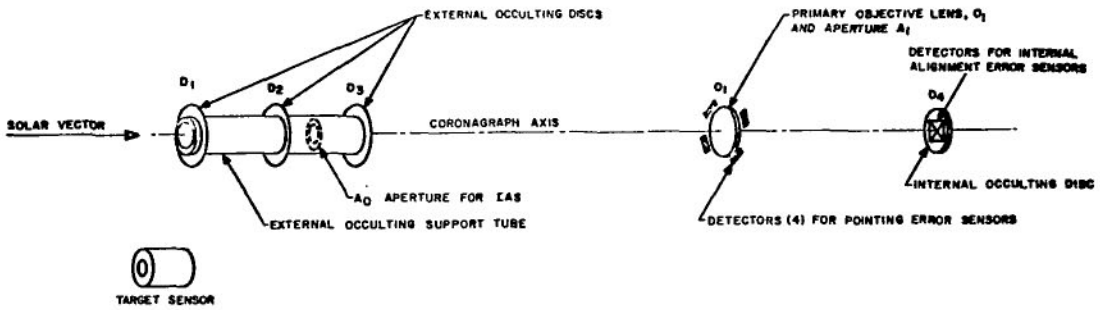

FIGURE 4. SCHEMATIC OF POINTING REFERENCE SYSTEM

Operational Background Information

From an operational standpoint, the experiment consists of external and internal shutters, pointing error sensors, internal occulting disk alignment error sensor, and the camera. Actual operation of the experiment consists primarily of actuating and monitoring the above four items, which are described below.

The external shutter protects the experiment from contamination and micrometeoric impact as well as protecting the front of the experiment from extreme heating from the heat dumping mirror when the ATM is in an offset pointing mode. The external shutter will automatically close when the coronagraph axis is pointed $\geq \pm 5$ arc min from the center of the sun.

A schematic diagram of the experiment pointing reference system is shown in Figure 4. The pointing error sensor consists of four silicon cells to detect the location of the shadow of the external occulting disks on the primary objective lens aperture. The outputs of diametrically opposed cells are subtracted and any asymmetry of cell illumination results in a cell output which is amplified and presented to the astronaut as the experiment pointing error. Breadboard tests of the system indicate the output is a linear function of the error angle over a range of $\pm$ 17 arc min, and the center pointing position (zero cell output) is repeatable to within $\pm$ 13 arc sec.

The internal occulting disk alignment error sensor functions electrically the same as the pointing error system. Optically, there is a target aperture in the tube of the external occulting disks that is imaged on the internal occulting disk by the primary objective lens. Direct sunlight enters the external occulting disk tube and is filtered by an infrared filter with low wavelength cutoff of 0.75 microns before passing down the system. Proper alignment of the internal occulting disk is accomplished by moving the disk until the infrared image is centered on the four silicon cells mounted on the internal occulting disk. Breadboard tests show the output of the system is a linear function of error angle over a range of ± 6 arc min, and the centering of the disk is repeatable to within ± 3.4 arc sec.

The experiment camera is a 35 mm sequential camera. The unit is sealed with an atmosphere inside to protect the film and mechanisms. Three cameras will be used in the mission, and all three will be preloaded with film. The camera will be capable of operating in the following four modes:

One-Minute Patrol Mode. — A camera shutter operate pulse shall occur every five seconds. The duration of the pulses which control exposure time shall sequentially vary from 1 1/2 seconds to 4 1/2 seconds to 1/2 second. After the complete sequence of three different shutter control pulses, the polarization wheel mechanism shall be automatically commanded to advance one position. The sequence of pulses shall repeat until all combinations of three shutter exposure times and four polarization wheel positions have been utilized. The camera programmer shall then stop automatically.

Sixteen-Minute Patrol Mode. — This shall be the same as the one-minute mode described above, except the sequence shall continue for 16 elapsed minutes.

Fast Scan Mode. — In this mode the shutter operate pulse durations will be approximately 1 1/2 seconds, 4 1/2 seconds and 1/2 second, and shall repeat cyclically in that order. A 1/2-second pause time shall occur between each pulse during the duration of the complete scan. The polarization wheel shall be driven to the clear position at the start of the fast scan mode and shall remain in this position during the nominal sequence of 16 minutes. The camera programmer shall automatically stop at the end of the sequence.

Long Patrol Mode. — In this mode the shutter operate pulse durations will be approximately 1 1/2 seconds, 4 1/2 seconds, and 1/2 second. Each shutter operation shall occur every 32 seconds, including shutter operation time, and shall repeat cyclically in that order throughout the duration of the complete scan. The polarization wheel shall be driven to the clear position while in the long patrol mode. The camera shall stay in the long patrol mode indefinitely or until a manual stop pulse is given.

XUV SPECTROHELIOGRAPH AND XUV SPECTROGRAPH (S 082A/S 082B, NAVAL RESEARCH LABORATORY)

By

G. M. Arnett

The Naval Research Laboratory (NRL) is contributing two experiment packages to the Apollo Telescope Mount Project (ATM). The two packages constitute one of the five major experiments on ATM. Principal Investigator and Principal Administrator for the NRL experiment are Mr. J. D. Purcell and Dr. R. Tousey.

The two experiment packages consist of a Coronal Extreme-Ultraviolet (XUV) Spectroheliograph (NRL-A) and a Chromospheric XUV Spectrograph (NRL-B).

Besides the two packages presently under preparation, NRL is considering more advanced versions of the two packages for a later ATM-type flight which, however, is not yet firmly planned. The two versions are referred to as ATM-1 and ATM-2. Actually, both the ATM-1 and the ATM-2 versions resulted from an earlier plan, listed in Table III under "August 1966."

The scientific objectives of the two NRL experiment packages will be discussed separately in the following sections.

The information contained in this section has been primarily abstracted from documents originating from NRL concerning the ATM program. Special use was made of the NRL/ATM proposal dated October 20, 1967, written by Mr. J. D. Purcell and Dr. R. Tousey of NRL.

Coronal XUV Spectroheliograph (NRL-A)

The objective of the spectroheliograph experiment is to record on film, at two separate times during the eleven-year sunspot cycle (ATM-1 and ATM-2), a large series of high spatial resolution extreme ultraviolet images in the range of 150 to 650 Å, covering periods of greater and lesser activity during two rotations of the sun during each flight, and obtaining spectra of developing centers of activity and of flares.

High resolution spectroheliograms made with visible and near ultraviolet radiation from ground-based observatories with flash spectra made during total eclipses of the sun are useful tools in studying the morphology of the lower chromosphere. The upper chromosphere and corona can be studied with high resolution spectroheliograms recorded with XUV radiation, which reaches altitudes planned for ATM but does not penetrate to the ground. Work of this type from rockets has established its importance, but is severely limited by the short exposure times, the small size of solar images, and the rocket pointing accuracy and jitter. With ATM, exposures ten or more times longer than with rockets are possible, large instruments producing large solar images with resolution not limited by photographic grain can be flown, and photographs can be obtained over a period of up to eight weeks to study changes in solar activity centers and the spectral and spatial history of flares. Hopefully this data can be obtained near sunspot maximum (ATM-1) and near sunspot minimum (ATM-2).

The spectroheliograph is complementary to the other experiments planned to be flown on ATM-1, since they will cover spectral regions on both sides of the spectroheliograph's range, including x-rays, longer wavelength XUV and visible light. Therefore, a record of a large portion of the spectral range from x-rays to visible light can be covered. For example, a limb flare may be recorded as producing a burst of plasma in white light by the High Altitude Observatory (HAO) coronagraph, as producing XUV resonance line emission by the spectroheliograph, and as producing emission from stripped atoms at extremely high temperatures by the Goddard Space Flight Center (GSFC) and American Science and Engineering, Inc. (AS&E) x-ray telescopes.

Photographic recording by the XUV spectroheliograph is essential to obtain quickly the required spatial detail before it changes and to record simultaneous images at different wavelengths. Specifically, the spectroheliograph will record monochromatic images of the sun in the emission lines in the

spectral range 150 to 650 Å. Among the most intense lines in this region in the quiet sun are Fe IX (171 Å), followed bv Fe X, XI, XII, XIII, XIV to Fe XV (284 Å) and Fe XVI (335 Å, 361 Å); He II (304 Å); Mg IX (368 Å); Ne VII (465 Å); He I (584 Å); and various lines emitted by O IV, V, and VI. These lines will provide information for the study of the corona and of the active regions of the chromosphere. Certain lines in this region, such as Fe XV at 284 Å and Fe XVI at 335 Å are enhanced considerably during flares. In addition, the information from the emission in this spectral region should contribute to the basic understanding of energy transfer processes, plasmas, and magneto-hydrodynamics. The sun is the only laboratory for the study of reasonably stable high temperatures, since the high temperature plasmas developed in earth laboratories are transient and subject to many limitations.

The spectroheliograph consists of a concave grating which will form images of the sun on XUV sensitive film (See Figure 5 for optical diagram.). The spectral range (150 to 650 Å) will be covered in two sections, each photographed separately, with the grating turned so that each section's center lies on the grating axis. The spectroheliograph will obtain monochromatic solar images 18.6 mm in diameter throughout the spectral range, with a dispersion such that the sun will cover about 24 Å along its diameter. Four film cameras will be utilized as the detector. Each film camera will hold 200 film strips, 35 mm by 258 mm in size, sufficient for 200 exposures. The astronaut is required to change film cameras by extravehicular activity (EVA) and to retrieve the final camera for return to earth. As is now planned, 800 exposures should be obtained throughout the mission.

Absolute pointing of the instrument is not required to better than one arc min. Stability during exposures to ± 2.5 arc sec, as provided by ATM, is essential for obtaining high spatial resolution. It is hoped that 1 arc sec spatial resolution can be obtained for the most intense features and spectral lines by using exposures short enough to stop the residual image motion caused by jitter of the ATM. Most of the exposures will be from 5 sec to 60 sec duration, with a few as long as five min. During a flare, exposures as short as 0.1 sec may be required. Actual exposure times will depend on the type of film used. This will be chosen after completion of the analysis of data from experiments on the effect of proton fogging on film and after analysis of the spectra to be photographed during 1968 from a rocket carrying the spectroheliograph.

The exposed film will be developed and studied by the Project Investigator and his colleagues. Study of the images will require making precise measurements of the positions, forms, and areas of various features with a comparator.

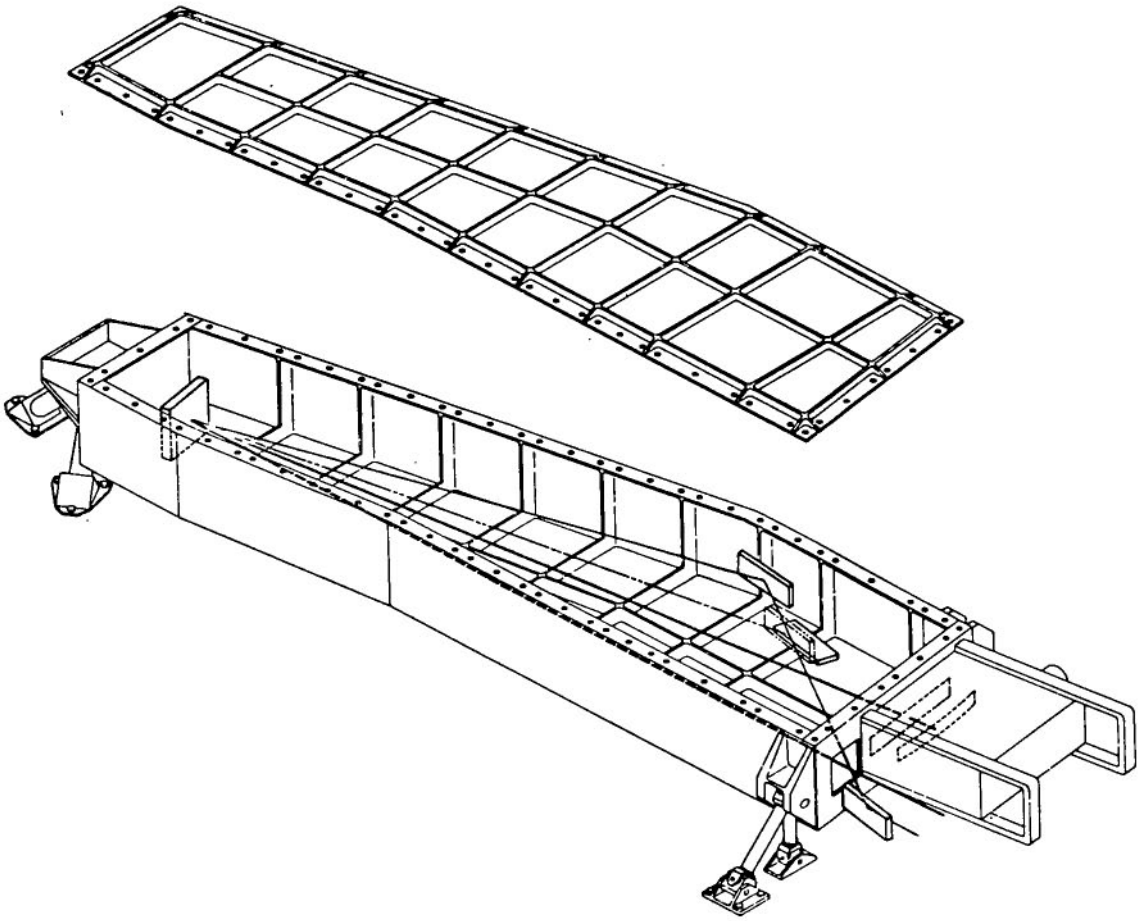

FIGURE 5. S 082A XUV SPECTROHELIOGRAPH

Intensity data will be obtained by using standard methods of photographic photometry employing microphotometers. Use may be made of contour-type microphotometers. Interpretations of the results will require study by many solar physicists who have had experience in the study of spectroheliograms made from ground-based observatories.

Chromospheric XUV Spectrograph (NRL-B)

As was mentioned earlier, the NRL-B experiment has been somewhat simplified for the ATM-1 mission and will be referred to as NRL-B-1; the

instrument as originally proposed will be referred to as NRL-B-2, which is proposed for ATM-2. For differences in the instrument's capabilities see Table III.

Extreme ultraviolet spectroscopic research from rockets and unmanned orbiting observations has demonstrated that knowledge of the sun's radiation in the spectra range from 3900 Å to x-rays will, in all probability, provide explanations for many perplexing solar phenomena, the most important being considered the solar flare. Although many significant results have been obtained, a great increase in spatial and spectral resolution, and also in knowledge of the changes with time, is required before satisfactory and complete interpretations and application to solve problems in solar physics can be made. In this regard, the advantages of ATM are obvious. (1) Photographic instruments can be used with their tremendous information recording capability. (2) Large instruments are possible, producing spectral dispersion and images large enough to be free from the limitations of photographic granularity. (3) An order -of-magnitude longer exposure can be made than in rocketborne instruments. (4) High spatial resolution and precise pointing can be achieved. (5) A large number of different instruments can be flown and operated simultaneously, or nearly so.

One of the most fundamental solar investigations involves determining the temperature profile, over the region where it becomes inverted. This is the most direct approach to learn how the process of energy transfer changes from convection to shock waves. This will be done by NRL-B by determining the intensity variation with height above the solar limb of spectral lines which originate from different parts of the entire transition region from the photosphere to the corona. One example is the D-lines in the Na isoelectronic sequence: Mg II 2795, 2803 Å; Al III 1855, 1863 Å; Si IV 1394, 1403 Å. The lithium sequence lines form a similar series. Step by step, the different lines originate from levels higher and higher above the photosphere until the corona itself is reached. Data of this sort have been obtained in one flight from a stabilized Skylark rocket by R. Wilson and W. M. Burton in England, but with far less spatial resolution than is required and at only one position above the limb. The difference between the spectra of the chromosphere and of the disk face-on is striking. The NRL-B-1 spectrograph will record off-limb spectra like the British, but with some 25 times greater spectra resolution. NRL-B-2, with twice the resolution of B-1, will record spectra automatically in steps of about 1500 km in altitude from the photospheric boundary (or below), through the steeply rising chromosphere and into the corona.

TABLE III. CHANGES OF PARAMETERS FOR NRL-B EXPERIMENT FOR ATM

Item	NASA-1138 Form of August 1966	ATM 1	ATM 2	Remarks
Spectral range	800 Å - 3000 Å (four steps)	970 Å - 1970 Å (2nd order) 1940 Å - 3940 Å (1st order)	970 Å - 1970 Å (2nd order) 1940 Å - 3940 Å (1st order)	
Spectral resolution	0.02 Å (1216 Å) 0.06 Å (2000 Å - 3000 Å)	0.08 Å (970 Å - 1970 Å) 0.16 Å (1940 Å - 3940 Å)	0.04 Å (970 Å - 1970 Å) 0.08 Å (1940 Å - 3940 Å)	
Spatial resolution (disk feature)	Not specified	4 arc sec slit (approx.)	2 arc sec slit (approx.)	
ATM stability	± 5 arc sec yaw, pitch; 20 arc min roll	± 2.5 arc sec yaw, pitch; ± 7.5 arc min roll	± 2.5 arc sec yaw, pitch; ± 7.5 arc min roll	
ATM shroud temperature	± 2.78° K (± 5° F) around an absolute value between 296-300° K (70-80° F)	Fixed between 289-296° K (60-70° F) with ± 1.67° K (± 3° F) variation	Fixed between 289-296° K (60-70° F) with ± 1.67° K (± 3° F) variation	
Slit length	20 arc sec and 60 arc sec	60 arc sec; not decided if 20 arc sec will be used	20 arc sec and 60 arc sec	
XUV monitor	No	Yes	Yes	Added in December 1966
Automatic limb pointing mode	Yes	No	Yes	
Cameras	2	3	3	Number has been raised to 4 in winter 1967, based on increase of mission length from 14 to 56 days
Film	Fast	Slow	Slow	Slow film necessitated by proton fogging
Flare prediction method	None	Magnetograph and/or existing ground H-α observatories	Magnetograph and/or existing ground H-α observatories	
Deliverable instruments	DVU, prototype flight, flight spare	TMU, prototype (refurbished as flight spare), flight	TMU, prototype (refurbished as flight spare), flight	
FDVU	No	Yes	Yes	Added in November 1966
ATM roll capability	Stated qualitatively	± 95 degrees	± 95 degrees	
Transmission to ground of XUV video picture	Not mentioned	1/orbit minimum	1/orbit minimum	
Mass	Total weight of A and B experiments estimated at 227 kg (500 lb)	181-224 kg (400-495 lb)	181-224 kg (400-495 lb)	
Power (avg)	Total average power for both A and B experiments estimated to be 10 W	14.2 W (spectrograph) 12 W (XUV monitor)	14.2 W (spectrograph) 12 W (XUV monitor)	
Exposures	At least 400	≥ 4800	≥ 4800	Each film strip is now designed to record 8 exposures
Predisperser gratings	4	2	2	
Absolute limb pointing accuracy	2 arc sec	± 2.5 arc sec (using ATM/FSS)	± 1 arc sec (using BBRC/PRS)	
External dimensions	269 × 48.3 × 30.5 cm (106 × 19 × 12 in.)	269 × 86.4 × 33.0 cm (106 × 34 × 13 in.)	269 × 86.4 × 33.0 cm (106 × 34 × 13 in.)	
Entrance windows	Approx. 7.6 × 7.6 cm (3 × 3 in.) and 12.7 × 12.7 cm (5 × 5 in.)	12.05 × 5.398 cm (4.745 × 2.125 in.) and 10 × 10 cm (4.0 × 4.0 in.)	12.05 × 5.398 cm (4.745 × 2.125 in.) and 10 × 10 cm (4.0 × 4.0 in.)	
Absolute disk pointing accuracy	5 arc sec radial	± 2.5 arc sec	± 2.5 arc sec	

Other features of interest in this study are the absorption continuum, which begins abruptly at about 2085 Å and extends to lower wavelengths. The details in this and the gradual disappearance of the Fraunhofer absorption lines, which becomes complete below 1500 Å, will also provide information on the energy mode change from convection to magnetohydrodynamic shock waves.

Few emission lines in the range 1000 to 3000 Å have yet been detected in the corona. This is a serious gap between the visible, where the forbidden coronal lines are found, and the range 1000 Å to x-rays where the coronal resonance lines occur. Both NRL-B-1 and B-2 have the capability of recording them.

A knowledge of the XUV spectra of the various features of the disk (e.g., the quiet regions, the features of the chromospheric network, and the centers of activity) is essential to understanding them and the processes by which they are created.

The study of flares, particularly in their formative phases (first few seconds) is of extreme revelance. Here there is a dearth of information. Hopefully, the XUV spectrum of a flare will lead to an understanding of these phenomena which have such an important effect on our terrestrial environment. This may also lead to increased protection against their harmful effects for the men and instruments in our future space probes.

The profile of the most intense XUV emission line, hydrogen Lyman alpha at 1216 Å, will reveal information about its origin in the sun. Also, its narrow absorption core should yield information about the cooler hydrogen surrounding the earth.

The more specific instrument-related scientific objectives can be broken down into five areas discussed below.

1. Spectra Across the Limb. Spectra will be recorded from different positions across the limb, from 12 arc sec inside the limb to 20 arc sec above the limb. These spectra will provide quantitative data on the change of physical conditions in the sun's atmosphere, passing from the photosphere through the transition layer to the chromosphere, and through the chromosphere into the corona.

The spatial resolution of B-1 will be sufficient to map the limb darkening of Fraunhofer lines as the limb is approached from below the photosphere, the

changes across the temperature minimum if it is rather flat, and the upper chromosphere-corona interface. From this, improved models of most of the transition regions can be developed. To map the bottom of the chromosphere, where the temperature rise is extremely sharp, will require the spatial resolution and accurate aiming of B-2.

2. Quiet Regions. NRL-B-1, although not equalling in spectral resolution the previously flown NRL rocket echelle, exceeds the latter in every other respect. The echelle provided data only for the central part of the sun. NRL-B-1 will record changes in Fraunhofer lines, and the various continua as the limb is approached. This is of great importance for deriving a complete and detailed photospheric model. During the 1967 International Astronomical Union Conference held in Bilderberg, the Netherlands, which was devoted to the photosphere and transition layer solar model, data of this kind were found to be greatly needed and essential. In addition, the spectra will be free from stray light, thus revealing the true depths of the cores of the many deep Fraunhofer lines and their change as the limb is approached. NRL-B-2, with its better spectral and spatial resolution and pointing, will be able to obtain profiles and changes in profile approaching the limb and follow the profile changes closer to the edge of the photosphere for many more lines than B-1.

3. Spectra of Special Features. When the sun is observed at 2 arc sec spatial resolution, there are many special features whose XUV spectra are of great interest: centers of activity, new versus old, the change in their spectra with time, and the change in their spectra when they approach and cross the limb; dark filaments, both central, near the limb, and at different latitudes; the different parts of the chromospheric network and supergranulation, observed both centrally and near the limb; and prominences, quiescent and active. The list could be continued, but it is obvious that even with two ATM missions this program cannot be completed. The B-1 instrument will be extremely valuable in accomplishing this; as a result, the selection of features to be studied by B-2 can be made with greatly increased knowledge.

4. Flare Spectra. The solar flare is certainly the most spectacular of solar events. Its XUV spectrum and the changes in its spectra from birth to disappearance is a primary objective. In the range of NRL-B the spectrum of a flare has never been recorded. NRL-B-1 offers the greatest chance of obtaining such a spectrum, because there will be more flares when ATM-1 is in orbit than a year or more later. Therefore, it is important to fly NRL-B-1, even though it will not provide as much spectral and spatial resolution as does B-2.

A problem is in pointing at the exact position where the flare appears. This touching-up of the pointing, through angles perhaps as great as 30 arc sec, must be done by the astronaut using the high resolution H-alpha telescope display. Such a display is planned for ATM-2 in Harvard College Observatory's "B" experiment (HCO-B), but as yet has not been arranged for ATM-1. Therefore, NRL-B-2 will obtain close to the ultimate in XUV flare spectral histories, provided a large flare occurs at the right time during the mission.

Although NRL-B-1 does not now have the possibility of precise real-time flare-pointing corrections, and may miss the interesting flare birth, it will have a far greater chance of securing spectra of a flare than B-2. The lesser spatial resolution of B-1 reduces somewhat its capability to determine temperatures and velocities through fine profiles and Doppler shifts. NRL-B-2 has this capability. And in this connection, improvements in flare prediction methods, onboard flare detection, and onboard prediction of flare importance after detection will greatly increase the chance of obtaining flare spectra with B-2.

5. XUV Monitor. The XUV monitor, to be flown in both ATM-1 and 2, will provide video pictures of the solar image in the spectral range of 170 to 550 Å, both to assist the astronaut in determining features of interest on the disk and hopefully to transmit to the ground (at least once per orbit) for further study and correlation. This range includes emission lines of highly ionized elements and thus allows observation of the corona above active centers and of flares in their hottest regions. Most importantly, it may show details, not visible in H-alpha, concerning how a flare is born.

Experiment Concept

The XUV chromospheric spectrograph NRL-B is a large double-dispersion, normal-incidence concave grating instrument with a wavelength range of 970 to 3940 Å covered in two steps (970 to 1970 Å and 1940 to 3940 Å). (See Figure 6 for optical diagram.) The NRL-B-1 instrument will have a spectral resolution of 0.08 Å in the range of 970 to 1970 Å and a resolution of 0.16 Å in the range of 1940 to 3940 Å. The NRL-B-2 instrument will have a factor of 2 better resolution, in both ranges, than B-1. The B-1 spectrograph will have a spatial resolution element of 3 arc sec by 60 arc sec, whereas the B-2 instrument will be variable to about 3 arc sec by 20 arc sec. The B-1 instrument will have a spatial resolution perpendicular to the slit of 4 arc sec when the ATM is stabilized. Through an internal stabilization mechanism, the B-2

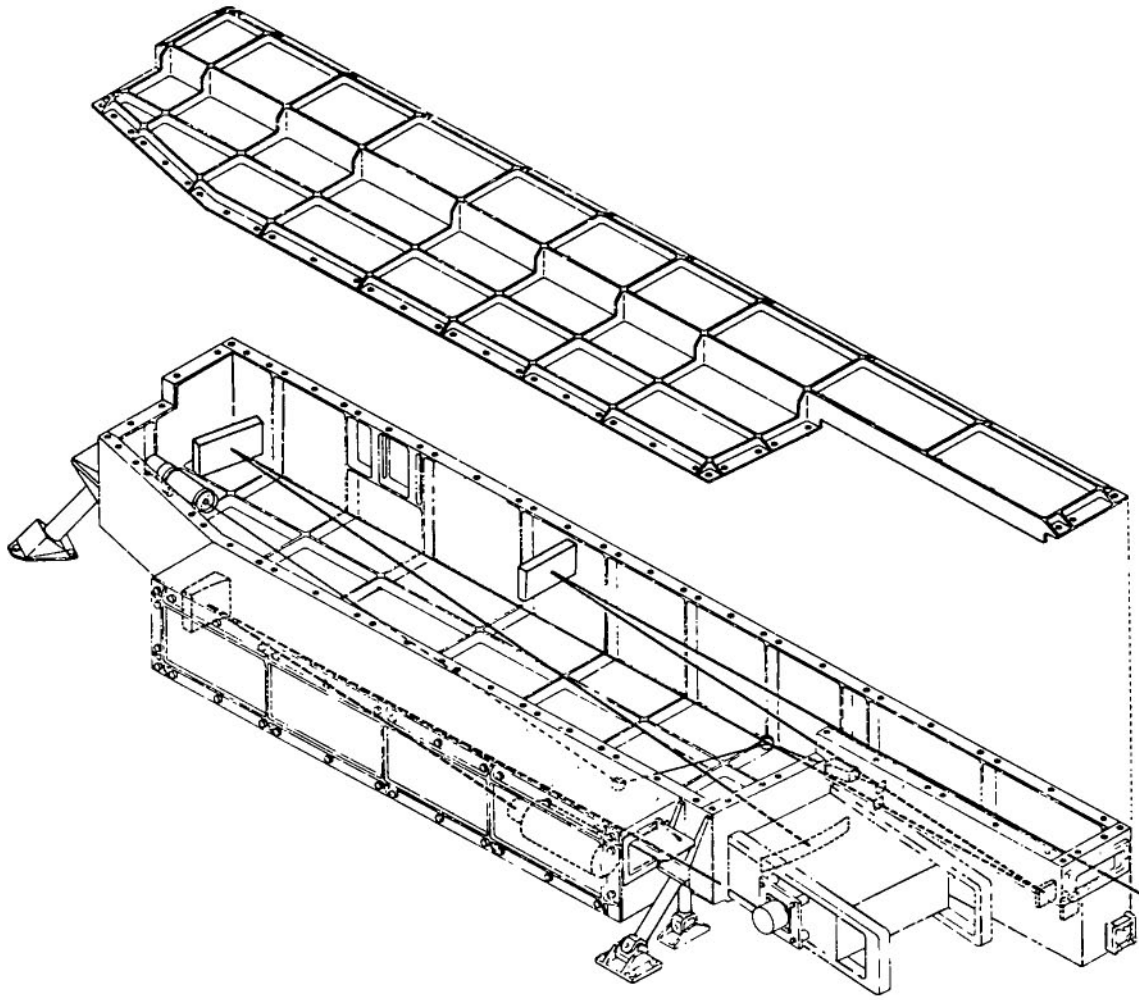

FIGURE 6. S 082B XUV SPECTROGRAPH AND XUV MONITOR

instrument will have a goal of spatial resolution perpendicular to the slit of ± 1 arc sec for limb scanning and ± 2.5 arc sec for disk features.

The spectrograph operates in four modes. The boresight mode will display a 3 × 3 arc min portion of the sun to the astronaut over closed circuit television in white light. It will be used when spectrograms of the central disk and of specific features near the limb are required and to acquire fine pointing to activate the limb scanning mode. In the boresight mode, a preprogrammed spectral sequence of photographs may be initiated in which four exposures in

each of two spectral regions will be made. The limb scanning mode will be used within 45 arc sec of the limb and will display a digital readout of the angular distance from the limb to the instrument optical axis in arc seconds. It will be used primarily to initiate the limb pointing mode, but can also be used in the spectral sequence of exposures. The limb pointing mode, used only in the B-2 instrument, will be used to make a series of exposures preprogrammed to cover ten discrete steps from 12 arc sec inside the limb to 20 arc sec off the limb. The fourth mode is the flare mode which will make 48 preprogrammed exposures of a flare when commanded by the astronaut. The capability also exists in the B-2 instrument to adjust the slit length in either of two positions. Exposures can be made manually in both instruments. For detailed differences in the B-1 and B-2 instruments see Table III.

As is now planned, there will be four film cameras allotted to this instrument. Each film camera contains 200 film strips which are 35 × 258 mm in size sufficient for 1600 exposures (each strip records eight exposures). Thus a total of 6400 exposures is planned. The astronaut will exchange the film cameras in the instrument and retrieve the final one.

Data reduction will be done much the same as that mentioned for NRL-A, except that NRL-B should lend itself more easily to computer methods.

X-RAY SPECTROGRAPHIC TELESCOPE (S 054, AMERICAN SCIENCE AND ENGINEERING)

By

Stanley A. Fields

The ATM-A experiment S 054 consists of an x-ray spectrographic telescope to study the soft x-ray emission of the sun during solar flares. The principal investigators are Dr. Riccardo Giacconi and Dr. William Reidy of American Science and Engineering, Inc.

The primary instrument consists of a grazing incidence telescope, a grating for spectral information, a filter wheel to vary the wavelength response, and a camera utilizing 70 mm format film to record the image.

A small telescope is used to focus an image onto a scintillator crystal which is in contact with the fiber optic faceplate and photocathode of the image dissector tube. The image dissector provides positional information on solar flare activity. The presence of an intense target on the cathode ray tube allows the astronaut to boresight the optical axis of the S 054 to the region of activity.

A photomultiplier detector is used as a flare detector and to provide exposure information for the camera shutter. In addition, the spectral shape of x-rays in the energy range of 5 to 100 keV is determined.

The proposal and other documents prepared by American Science and Engineering, Inc. (AS&E) in support of this project were used in preparing this report.

Scientific Background

The sun was discovered to emit x-rays in 1948 by Burnight.[1] Since that time, observations in the x-ray region of the spectrum have been made by both direct and indirect means.

---

1. T. R. Burnight, Physical Review, Vol. LXXVI (1949), p. 165.

X-rays are indirectly observable through the sudden ionospheric disturbances produced by their absorption and consequent increased ionization of the upper layers of the earth's atmosphere. They have also been directly observed from rockets and satellites. The observation of ionospheric phenomena can provide only qualitative information on flare x-ray emission. Direct observations of flare x-ray emissions have been made by the NRL group, the University of London and Leichester group and the GSFC group.[2] The detectors used have been of the broad band type consisting of thin window Geiger-Mueller counters, proportional counters, and ionization chambers for the soft x-ray spectral region ($\lambda > 2$ Å), and scintillation counters for the harder x-ray region. This work has been summarized as follows:[3]

1. Solar flares have been observed to be accompanied by a considerable enhancement of the x-ray emission and a hardening of the spectrum. Solar x-rays of wavelengths less than 5 Å have been observed only in association with solar flares.

2. In individual cases, the intensity, the spectral characteristics, and the temporal variations of the x-ray emission were found to exhibit clear correlations with the development of the flare as observed in the visible and radio region of the spectrum. The type correlation, however, is not always the same.

3. Two different processes of x-ray emission appear to be associated with solar flares. The first gives rise to x-rays, which gradually increase in intensity and are comparatively soft yet somewhat harder than those observed during nonflare conditions. The second gives rise to a burstlike emission of x-rays, with a spectrum extending usually into the hard x-ray region. Bursts of x-rays up to 500 keV have occasionally been observed in connection with solar flares. There is evidence that the burstlike emission is associated with the large flares and with the flash phase of H-α flares.

Concerning the interpretation of the observed phenomena, it appears that the first emission process may be explained by an increase in the density or the temperature of a portion of the solar atmosphere; therefore it should be classified as a thermal emission. The second emission process is believed to be due to the sudden acceleration of electrons; this should be classified as a nonthermal emission.

---

2. Design and Performance Specification, ATM Experiment S 054, ASE-1600-A, October 1, 1967.

3. Ibid.

In addition to flare-associated x-rays, there is a considerable x-ray flux associated with solar centers of activity, or plage regions, and the general solar corona. This radiation is generally attributed to emission from a hot thermalized coronal plasma with a temperature on the order of a million degrees.

Thermal Process

In the case of a thermal process, the electrons have a Maxwellian energy distribution. The x-ray emission originates from free-free transitions (continuous spectrum), from free-bound transitions (continuum and edge discontinuities), and from bound-bound transitions (line spectrum). The relative importance of these processes will depend on the physical conditions prevailing in the source region. In particular, the intensity of the line spectrum is determined by the abundance of heavier elements (such as O, Si, Fe) that are not completely ionized at the existing temperature.

Nonthermal Process

In nonthermal processes, emission is due to electrons with average energy much greater than the average energy of plasma particles. The x-ray spectrum will depend on the composition of the plasma, and in an essential manner, on the energy distribution of the electrons determined by the acceleration mechanism.

The best observations on the spectral characteristic of the x-ray emission from solar flares are those made by Culhane et al.[4] They used proportional counters to obtain low resolution spectra of x-ray emissions associated with flares. Their results show a gradually increasing x-ray component associated with Class 1 flare, and the spectral development of the burstlike x-ray component associated with a Class 2 flare. The results clearly show the enhancement at short wavelengths occurring during solar flares. A comparison of the enhancement with the quiet sun condition indicates that the spectral range from 2 Å to 8 Å is suitable for the observation of flares. The flux level at 6 Å, in the case of the Class 1 flare, shows an enhancement of greater than ten over the quiet sun, while at the same time

4. J. L. Culhane et al., Space Research IV, ed. P. Muller (Amsterdam: North Holland Publishing Co., 1964), pp. 741-759.

reaching an absolute value of 3×10^{-4} ergs/cm^2-sec-Å. This is adequate to provide good spatial, temporal, and spectral resolution with the S 054 instrument.

The analysis of the dispersed spectra, with the resolution obtainable in the AS&E experiment, is expected: (a) in the case of the thermal process, to indicate the mechanism (or mechanisms) responsible for the x-ray emission; (b) in the case of nonthermal processes, to provide information on the generation of nonthermal electrons up to energies of tens of thousands of electron volts in the solar atmosphere.

Spatial Resolution

Observations of x-ray flares performed in the past gave only the integral flux, and did not attempt to determine the spatial distribution of the x-ray emission. A detailed knowledge of this distribution makes it possible to determine the volume of the emitting region and afford an independent estimate of the electron density. Furthermore, observations of the structure of the x-ray emitting region and of the temporal changes of the intensity allow a direct comparison with corresponding visible light and radio observations. It is expected that these observations will further the understanding of the mechanisms involved in flare energy storage and its subsequent sudden energy release. In particular, the following points will be clarified: (a) the role of the magnetic field in controlling the initiation and evolution of the phenomenon, (b) the importance of neutral points in the magnetic field as a triggering mechanism, and (c) the preferential association of flares with chromospheric plages and sunspot groups.

Scientific Objectives

The primary purpose of the S 054 experiment is to study solar flare emission in the soft x-ray wavelengths with a spectral resolution of a fraction of an angstrom and a spatial resolution of 2 arc sec. The instrumentation (Figs. 7, 8) consists of an x-ray transmission grating combined with a grazing incidence telescope and combines the dispersive properties of the grating with the imaging properties of the telescope. This experiment has the capability of simultaneously imaging the emitting region and recording the soft x-ray spectrum. The secondary objective of the experiment is to obtain soft x-ray images of the sun during nonflare conditions using either transmission filters or the transmission grating.

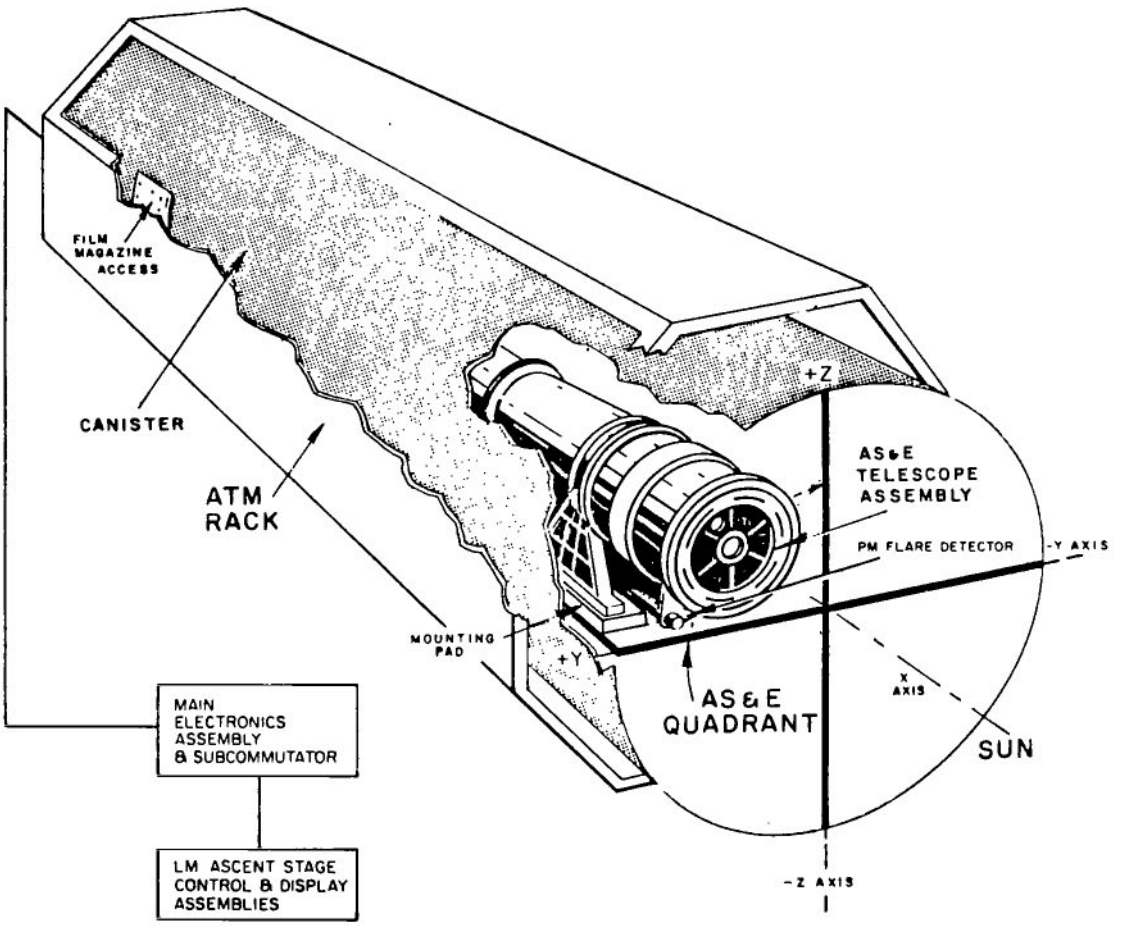

FIGURE 7. S 054 MECHANICAL ASSEMBLY

The large grazing incidence mirror consists of two coaxial mirrors of the paraboloid-hyperboloid configuration (Figs. 9, 10). The inside diameters of the mirrors are approximately 22.9 and 30.5 cm (9 in. and 12 in.). The total collecting area of the mirrors is 42 cm^2. The focal length is 213.4 cm (84 in.). The field of view of the telescope is 48 arc min.

Aperture plates are attached to the front and rear flanges of each mirror (Fig. 11). The transmission gratings are placed behind the rear aperatures of the mirror assembly where they disperse a portion of the incident radiation, thereby producing a dispersed image in the range

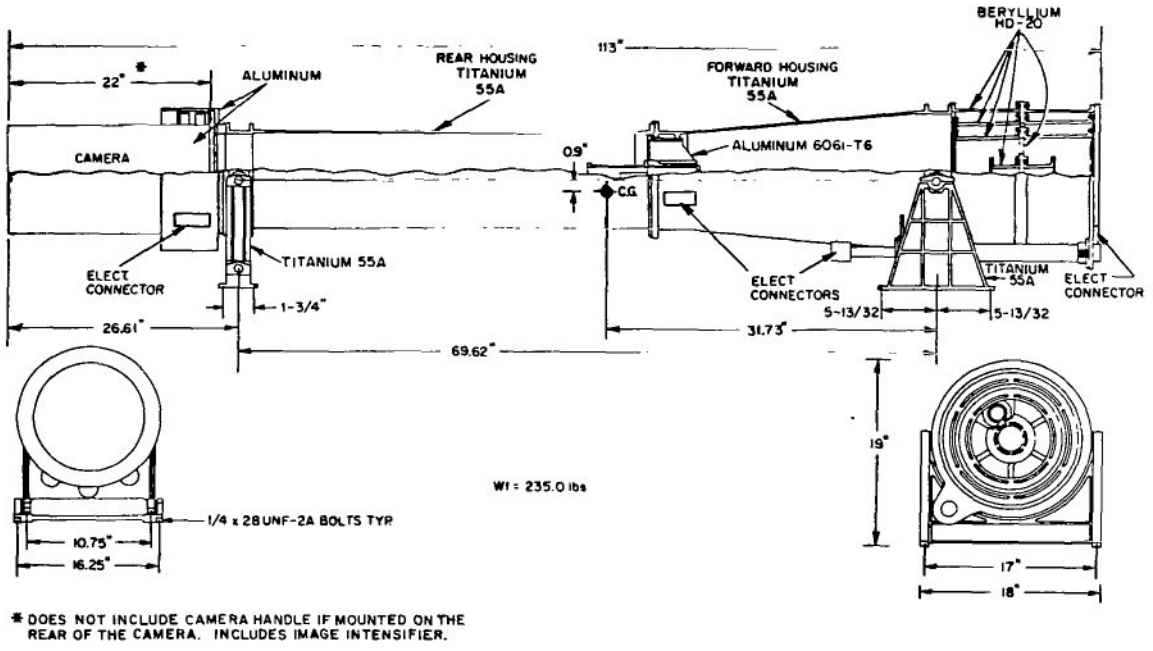

FIGURE 8. TELESCOPE ASSEMBLY

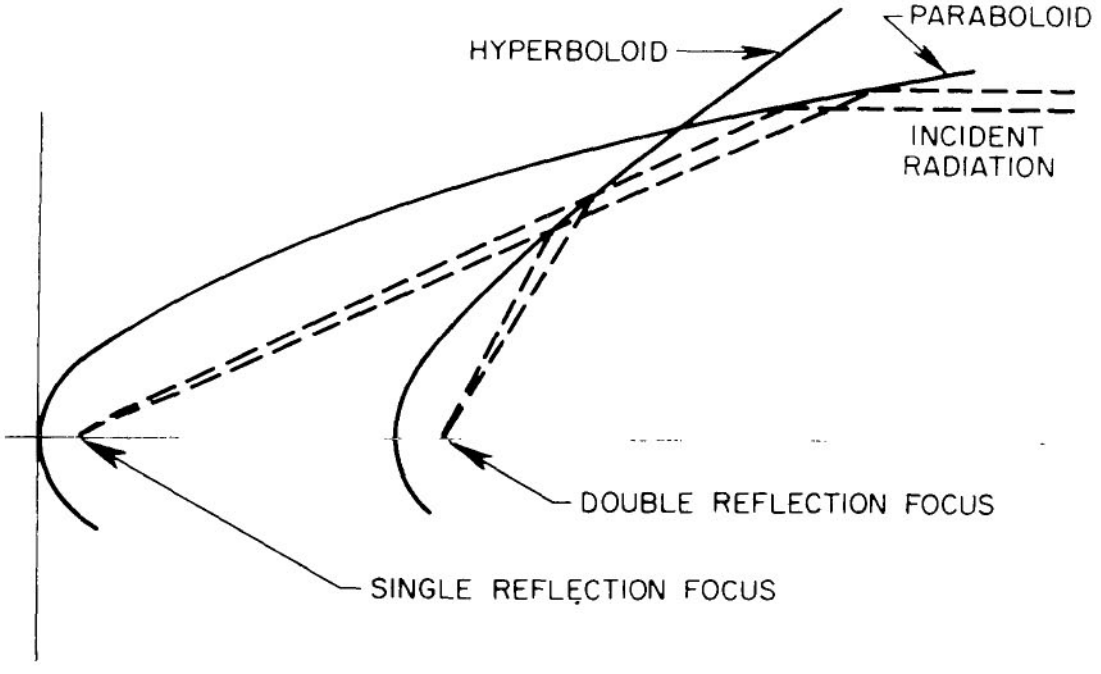

FIGURE 9. SCHEMATIC CROSS SECTION OF X-RAY TELESCOPE

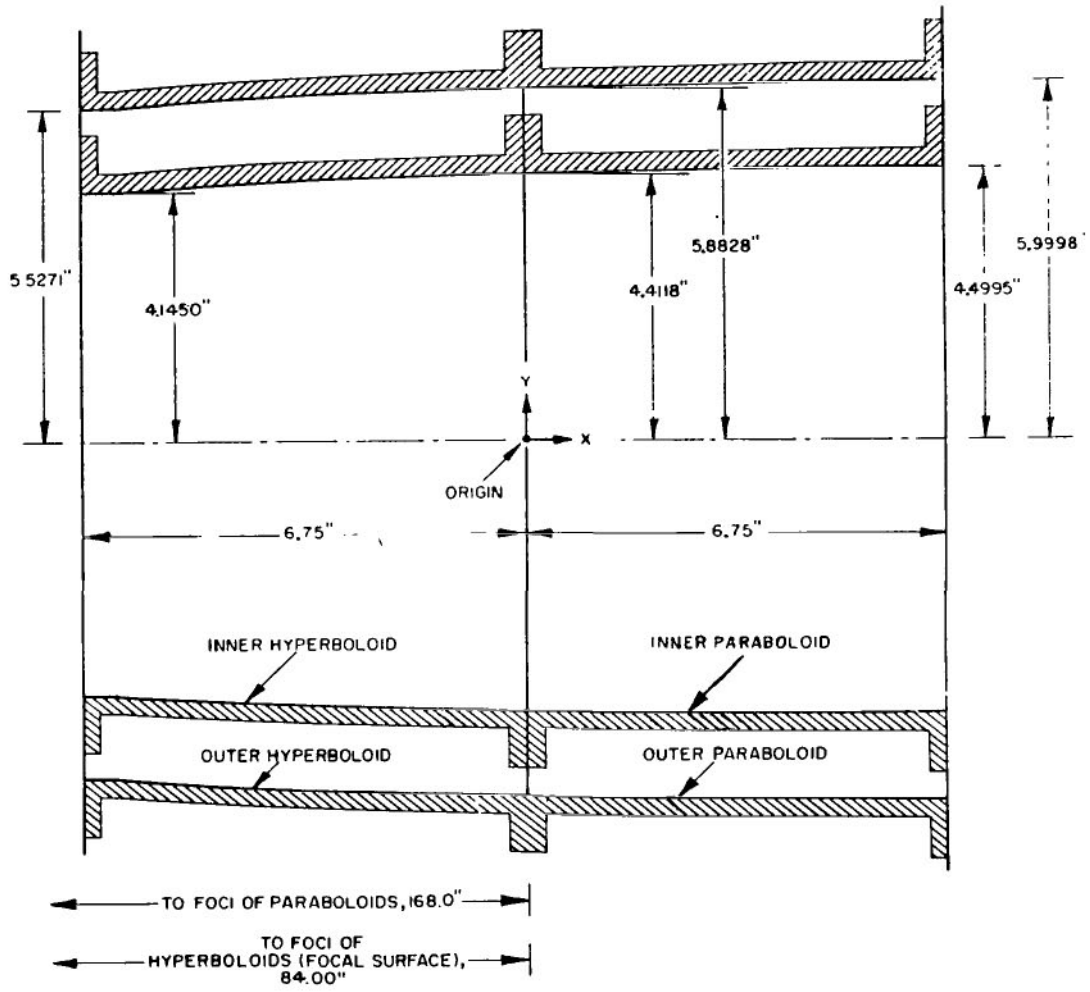

FIGURE 10. LARGE TELESCOPE DESIGN

2 to 8 Å with a spectral image of at least 0.5 Å (Fig. 12). The grating is mounted so that it can be moved out of the path of x-rays to allow observations without spectral dispersion.

A filter wheel is located in front of the film plane. Six filters are selected and mounted in the rotating wheel to vary the wavelength response of the instrument. The filters to be used are as follows:

1. Two 0.00127 cm (0.0005 in.) Be filters. One of these is the "normal" filter for use with the diffraction grating and the other is considered a spare.

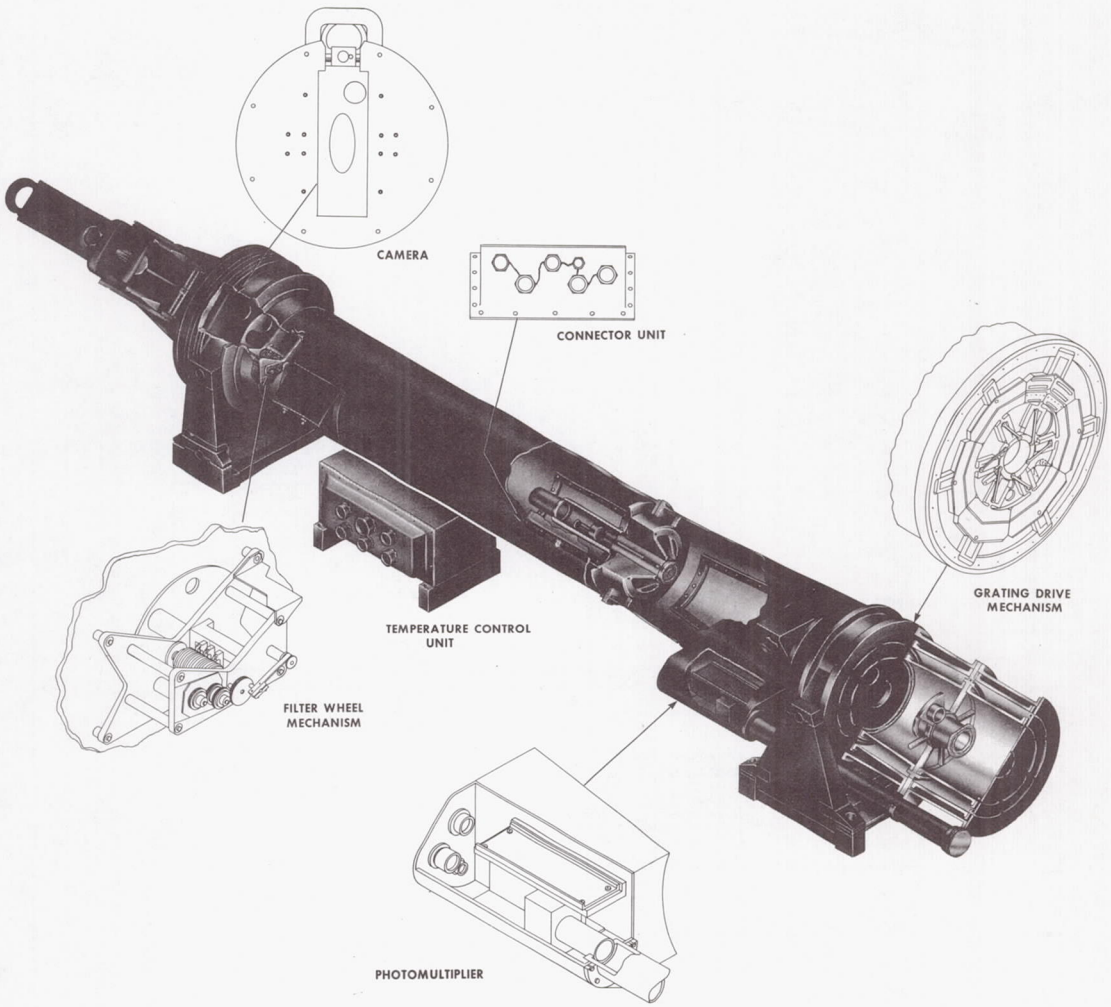

FIGURE 11. S 054 TELESCOPE ASSEMBLY

2. One 0.0051 cm (0.002 in.) Be filter for observations out to 10 Å.

3. One thin organic filter, such as 0.00038 cm (0.00015 in.) Mylar and 2200 Å Al filter for quiescent mode operations in the 44 to 60 Å region.

4. One 0.000635 cm (0.00025 in.) Al filter for 8 to 20 Å or one 0.00254 cm (0.001 in.) Be filter for 3 to 16 Å.

5. A neutral density filter for a visible light solar image.

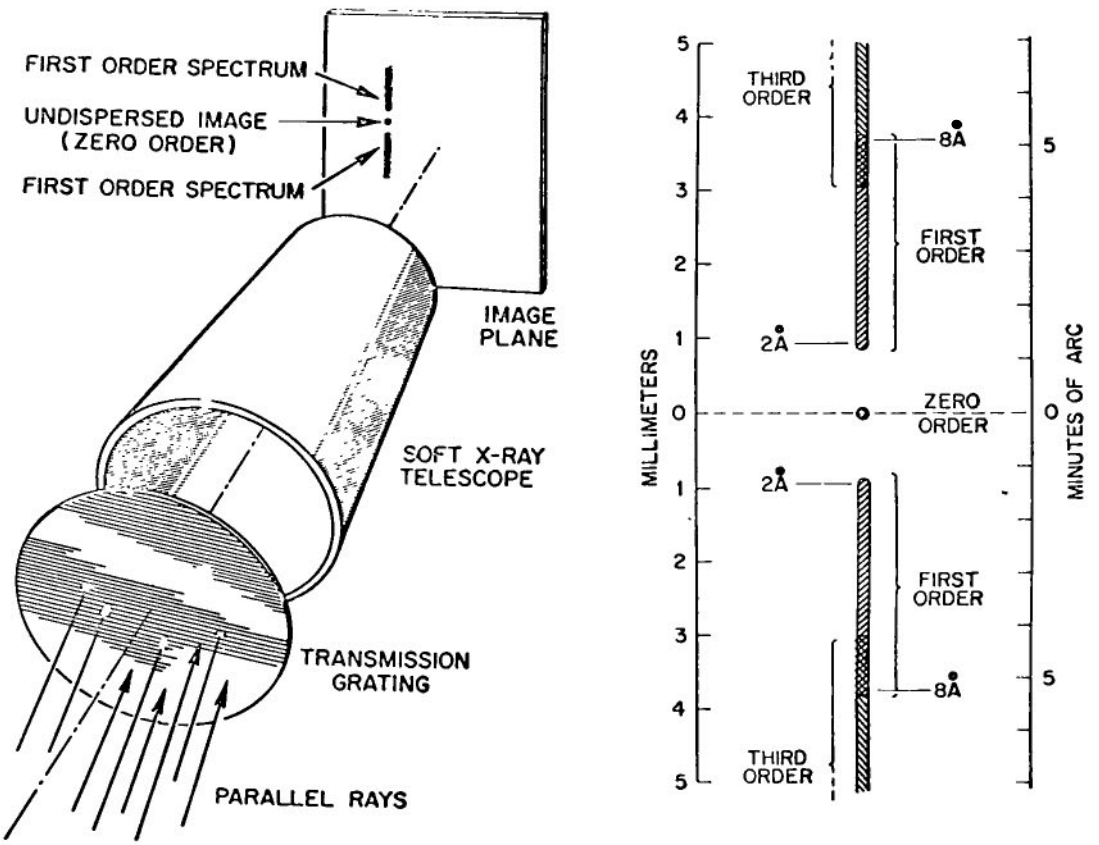

FIGURE 12. SLITLESS SPECTROMETER

The x-ray image will be recorded on film of 70 mm format in 1000 ft rolls. The film magazine will be changed every 14 days. The camera shutter speeds can be automatically or manually controlled from 1/64 to 256 sec in the following increments: 1/64, 1/16, 1/4, 1, 4, 16, 64, and 256.

The film will contain the following information for each exposure:

1. Time at which exposure begins
2. Duration of exposure
3. Grating position
4. Filter position

The 7.62 cm (3 in.) diameter telescope has a focal length of 91.4 cm (36 in.) and a collecting area of 2.1 cm^2. This telescope focuses a filtered image on a scintillator crystal which is in contact with the fiber optic faceplate and photocathode of the image dissector tube. The output of the image dissector tube is gated into the intensity counter. The output from the intensity counter is displayed on the cathode ray tube when a given threshold is exceeded. It is also displayed as a three-digit readout on the control and display panel. Figure 13 is a schematic of the assembly.

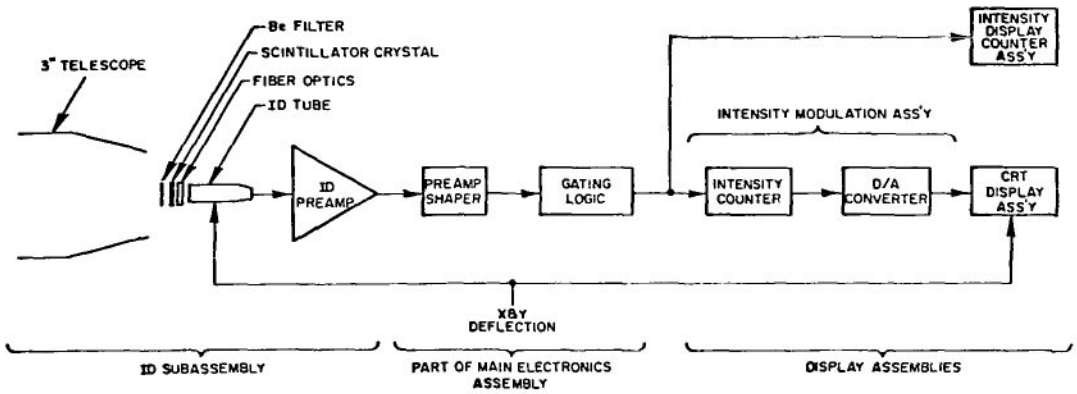

FIGURE 13. SCHEMATIC OF 7.62 cm (3.0 in.) TELESCOPE ASSEMBLY

A photomultiplier detector is used to measure the x-ray intensity. When a preset discriminator level is exceeded, an x-ray alarm is energized. The photomultiplier detector also provides exposure information and is numerically displayed as a three-digit number on the control and display panel. In addition, the spectral shape of x-rays in the energy range of 5-100 keV is determined. Figure 14 is a schematic of the assembly.

The visible light lens with a clear aperture of 4.5 cm (1.75 in.) and a focal length of 213.4 cm (84 in.) will be used to produce a solar image 1.9 cm (0.757 in.) diameter. A neutral density filter will be used so that the film will receive an optimum exposure at a fixed shutter speed of 1/64 sec. The camera will have a visible light shutter separate to the x-ray shutter.

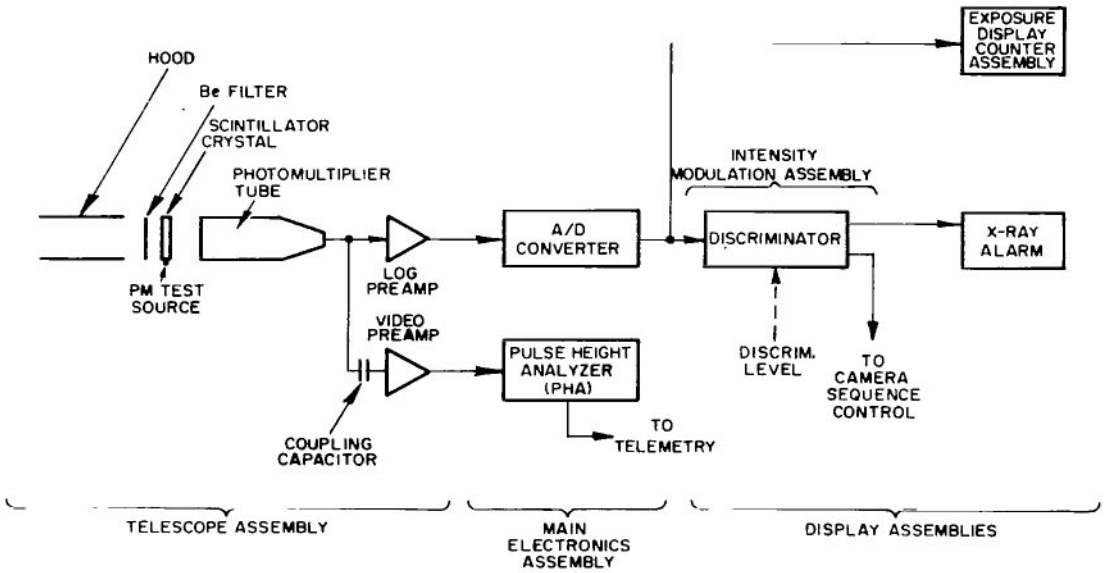

FIGURE 14. SCHEMATIC OF PHOTOMULTIPLIER DETECTOR ASSEMBLY

In summary, the objectives of this experiment are as follows:

1. Obtain images of the x-ray flare event with a spatial resolution of a few seconds of arc.

2. Simultaneously record flare spectra over the range of 2 to 10 Å with a spectral resolution of a fraction of an angstrom; in particular, to detect the presence of lines (or groups of lines) and the continuous spectrum.

3. Follow the evolution of the spatial image and spectral distribution during the onset, development, and decay of a flare with a time resolution of approximately 1 sec.

4. Correlate these measurements with ground-based radio and H-α measurements for the purpose of constructing a comprehensive picture of solar flare phenomena.

5. Perform similar measurements during nonflare conditions; study the active solar region; and determine the relation between centers of activity and flare events.

ULTRAVIOLET SPECTROMETER (S 055A, HARVARD COLLEGE OBSERVATORY)

By

Ed Klingman

The Harvard College Observatory (HCO) Experiment to be flown on the Apollo Telescope Mount (ATM) mission consists of a short wavelength spectroheliometer to take intensity measurements of the sun in the ultraviolet spectrum. The S 055A instrument operates in the 300 to 1400 Å region with a five arc second spatial resolution and a spectral resolution of about 1.3 Å. A 60 line spatial scan is performed to build up a 5 arc minute square picture. Eight (8) discrete spectral lines are singled out and monitored by eight separate detectors. There is also a movable grating which spectrally scans the entire spectral region. An H-α telescope is included for pointing control and also to provide photographic records at a wavelength of 6563 Å. The primary objective of the experiment is to observe the evolution of solar flares simultaneously in many characteristic lines.

Solar radiation emanates from the three regions of the sun shown in Figure 15: the photosphere, chromosphere, and corona. The extreme thermal gradient in the chromosphere gives rise to turbulent convective processes. Rising and falling columns of plasma at 4000° K to 30 000° K are called granulations and supergranulations. Plasma spicules are also present and can be seen in solar eclipse. The radiations from the hot chromosphere and corona regions are in the extreme ultraviolet spectrum and are completely blocked by the earth's atmosphere. For this reason large scale perturbations in the chromosphere such as sunspots (cool), plage regions (hot), and flares are little understood. The tremendous effect of these disturbances on the earth's atmosphere makes it desirable to obtain more information from wavelengths characteristic of this region in order to develop models of thermal, electromagnetic, and atomic processes occurring in the chromosphere.

The discrete spectral lines monitored by the Harvard instrument correspond to excitation energies ranging from 10 eV to 24 eV. The limb darkening profile should be quite different over this range of excitation energies. Thin lines such as Ne VIII should show a thin ring of brightening at the limb while thicker lines will have different center-to-limb variation. This is illustrated in Figure 16.

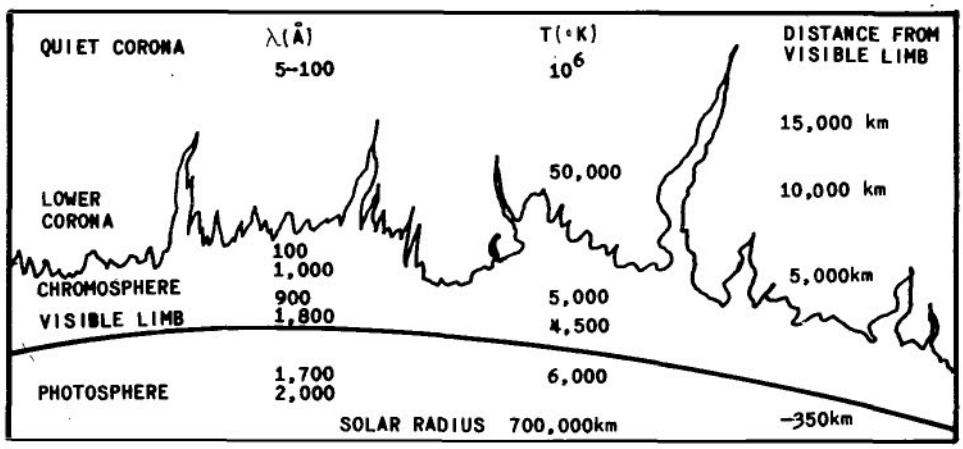

FIGURE 15. RADIATIVE REGIONS OF THE SUN

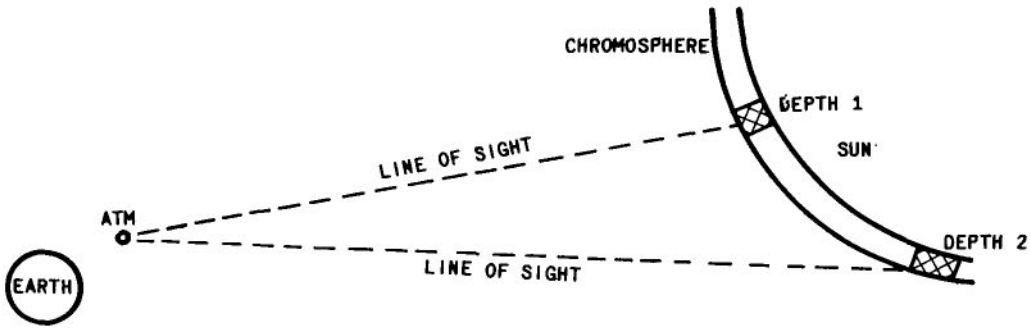

FIGURE 16. MEASUREMENT OF CHROMOSPHERE

The order is such that highly ionized lines should be systematically displaced toward the limb relative to the less highly ionized lines due to the projection of the considerably different heights of formation of these lines. If the Si XII lines are formed at $10^{6\circ}$K, from Figure 15, we see that the apparent solar radius should be 10 000 km or 15 arc sec larger than in hydrogen. Measurements of the width and intensity of the thin ring of brightening will yield information on the density distribution of ions in the corona, and from this data a determination can be made of the density structure and temperature of the low corona. For optically thick lines like Lyman (λ 1216), He I (λ 584), and C III (λ 977), this brightening should be less extreme and should heavily reflect the spicular structure. The five arc sec resolution should yield information about the spicules and inter-spicules material, even if only the very largest spicules are resolved. The

high resolution should also allow measurement of the temperature and density changes across the boundaries between regions of supergranulation. There is some evidence from calcium emissions that the size of the emission region at the boundaries increases with height. Such observations can be made at the higher energies O VI, Ne VIII, and Mg X. Similar measurements should add information indicating that plage regions in Lyman-α exist to a greater extent than those observed in calcium K. This shows up even more at higher energies. Simultaneous measurements of Lyman-α, H-α, and the Lyman continuum should contribute to studies aimed at determining whether certain intensity changes result from temperature changes or changes in abundance. In the region discussed above, i.e., < 1300 Å, there is little continuous background, mostly discrete emission lines. From intensity profiles of the continuum will come much valuable information about the transition region between the photosphere and chromosphere. Such information is necessary for the study of chromospheric heating mechanisms.

The following lines will probably be monitored:

O IV	554	C III	977
Mg X	624	O VI	1032
Ne VIII	(spare) 770	H Lyman	1219
Lyman cont.	896	C II	1335

Experiment S 055A Instrument Description

The S 055A instrument will perform the following primary functions:

a. image a portion of the collected solar energy on the entrance slit of a spectrometer

b. diffract the solar radiant energy passing through the spectrometer entrance slit and image the diffracted slit images on seven exit slits

c. simultaneously measure the intensity of the U. V. at each of seven preselected spectral regions.

d. The primary mirror will provide a five arc min raster scan of selected regions of the solar disk with five arc sec spatial resolution. A single scan of any line will be possible. The scan velocity will be 1 arc min/sec with nominal raster scan time of 5.5 min.

e. The diffraction grating may be rotated to permit wavelength scan or to select a desired wavelength with 1.3 Å spectral resolution. The grating will be mounted in a Johnson-Omaka type mount.

Other specifications are:

a. Reflective elements will have a minimum reflectivity at normal incidence of 90 percent at 5461 Å.

b. The grating will be Au coated with a minimum 10.41 cm^2 (1.615 $in.^2$) ruled area with 1800 lines/mm. The linear dispersion will be 11.2 Å/mm.

c The grating scan range will be 300 to 1336 Å with a scan rate of 3.6 min/scan. The scan steps will be 0.2 Å at 24 steps/sec for an integration time of 0.041 sec. The scan will be unidirectional in the direction of decreasing wavelength.

d. The detectors will consist of seven (plus one spare) channeltron photomultipliers. The unit will be open faced and therefore the environmental pressure will be critical to prevent arcing.

Optical Paths

As shown in Figure 17, collimated light passes through the entrance aperture and impinges upon the primary (movable) telescope mirror. It is reflected by this first surface parabolic mirror and focused on the entrance slit mirror of the spectrometer. The light from the region of interest (a five arc sec square selected region of the solar disk) enters the spectrometer via the entrance slit and is diffracted by the grating to focus each wavelength on the Rowland circle (shown in Fig. 18). The intensity of the light as a function of wavelength is measured by detectors by scanning the grating as the seven preselected spectral regions are monitored. The solar image on the entrance slit is reflected to heat rejection mirrors which reflect the light back out through the entrance aperture.

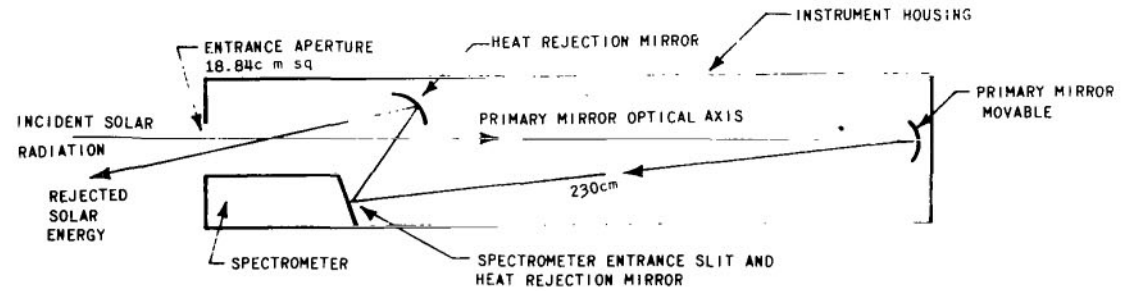

FIGURE 17. SIDE VIEW OF S 055A EXPERIMENT

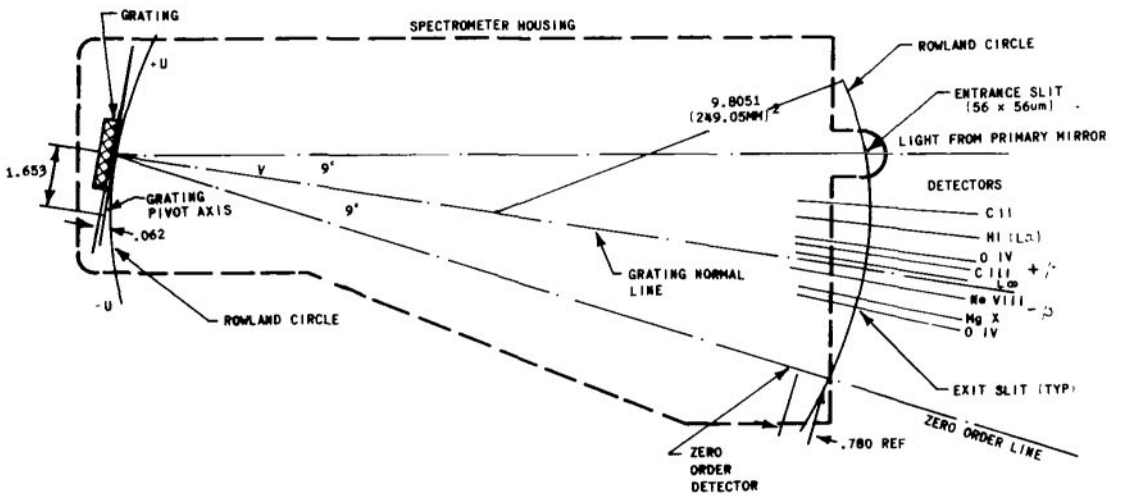

FIGURE 18. S 055A SPECTROMETER

Orientation

The orientation of the five arc sec square region of the solar disk will be determined as follows. The movable primary mirror will be locked in a stow position and the grating will also be placed in a reference (zero order) position. The instrument will then be moved across the limb of the sun until a zero order indication is obtained. The instrument pointing axis will then be correlated to the sun seeker axis and future HCO pointing information will be obtained from sun seeker information through telemetry.

Mode of Operation

The primary objective of the S 055A instrument is to obtain both time and spatial evolution of solar flares in many characteristic lines. The ability to select single spatial scans and to select arbitrary wavelengths increases the flexibility of the instruments and allows numerous secondary objectives. By preselecting a certain atomic emission line the rapid time change of this line can be continuously monitored. During quiet sun condition, a program of measurements of a series of well defined positions on the disk and in the coronal region will be conducted to obtain "typical" quiet sun characteristics.

X-RAY TELESCOPE
(S 056, GODDARD SPACE FLIGHT CENTER)

By

Anthony de Loach

Considerable information regarding the physical state of the solar corona can be obtained from observations in the soft x-ray region. These data will help to give a better understanding of mass and energy transfer mechanisms, and of the initiation and temporal development of solar flares. Within the 5 to 60 Å wavelength region, the Goddard instrument will obtain spatial and temporal distributions of x-ray sources over the solar disk and beyond the limb to approximately 1.5 solar radii.

The x-ray emission from the sun can be conveniently divided into three principal components: (1) emission from the quiet corona at times of no solar activity, or from undisturbed areas distant from active regions; (2) a slowly varying component from active regions in the corona above phenomena such as sun spots and plages; (3) rapidly varying x-ray bursts which may or may not be associated with solar flares, eruptive prominences, or radio bursts. Within each of these categories, several problems of interest in modern solar physics are proposed for investigations that are listed below.

Quiet Sun Emission

1. Electron density and temperature in regions far from active centers.

2. Relationship of the quiet sun emission with solar magnetic field as evidenced by polar darkening and the appearance of x-ray filaments, plumes, and arches.

Active Region X-Rays

1. The size, shape, electron density, and temperature of x-ray emission associated with active regions. Correlation with visible light spectroheliograms, white light, and ultraviolet coronagraph data, magnetic data.

2. Variation of the size and height of the coronal emission with excitation energy of the radiation observed.

Rapidly Varying Bursts

1. The processes occurring during the initial stages of flare development. The relationship between flare development in the x-ray, H-α, and radio regions.

2. The correlation between the importance of a flare and the x-ray burst intensity.

3. Temporal and spectral correlations between x-ray bursts originating from flare versus nonflare sources.

4. The role of local magnetic field strengths and gradients in triggering and sustaining flare development.

The spatial information required to satisfy the scientific objectives will be in the form of filtergrams, utilizing a grazing incidence paraboloidal/hyperboloidal mirror system, several metal and plastic bandpass filters, and x-ray sensitive film. Supplementing the solar images, the spectral distribution of the x-ray flux between 2 and 20 Å will be provided by two proportional counters, the pulses from which are input to and sorted by pulse-height analyzers.

Experiment Description

This section defines the scientific need and methods for the S 056 Extreme Ultraviolet X-Ray Telescope experiment.

The purpose of this experiment is to gather data which will help give a better understanding of the physical processes occurring in the solar atmosphere; primary emphasis being placed on transient solar events such as solar flares. To date, a significant quantity of data has been obtained on the time dependence of the spectrum of solar flares (and other transient phenomena) from the γ-ray region out to the radio region. However, data on the structural changes of the emitting regions in the ultraviolet and x-ray regions is nonexistent because of limitations of the various observing techniques previously available.

This experiment will provide crude spectral data using proportional counters and pulse-height analyzers and spatial data in the form of x-ray filtergrams (solar images of narrow wavelength intervals). The spectral data will be analyzed to give flare temperatures, densities, and chemical abundances. The filtergrams will indicate both the temporal and spatial variations of these quantities in the flare region.

The strong nonthermal x-ray emission characteristic of flares will be used to gain more understanding of the plasma instabilities and their influence on flare development. This understanding should lead to more definite relationships between sunspots and flare formation. Of particular interest will be the processes occurring during the initial stages of flare development and the relationship between flare development in the x-ray, H-α, and radio regions.

The spatial information required to satisfy the objectives can be obtained with a grazing-incidence telescope system, and the spectral information with proportional counters (Fig. 19), particularly for events of limited spatial extent.

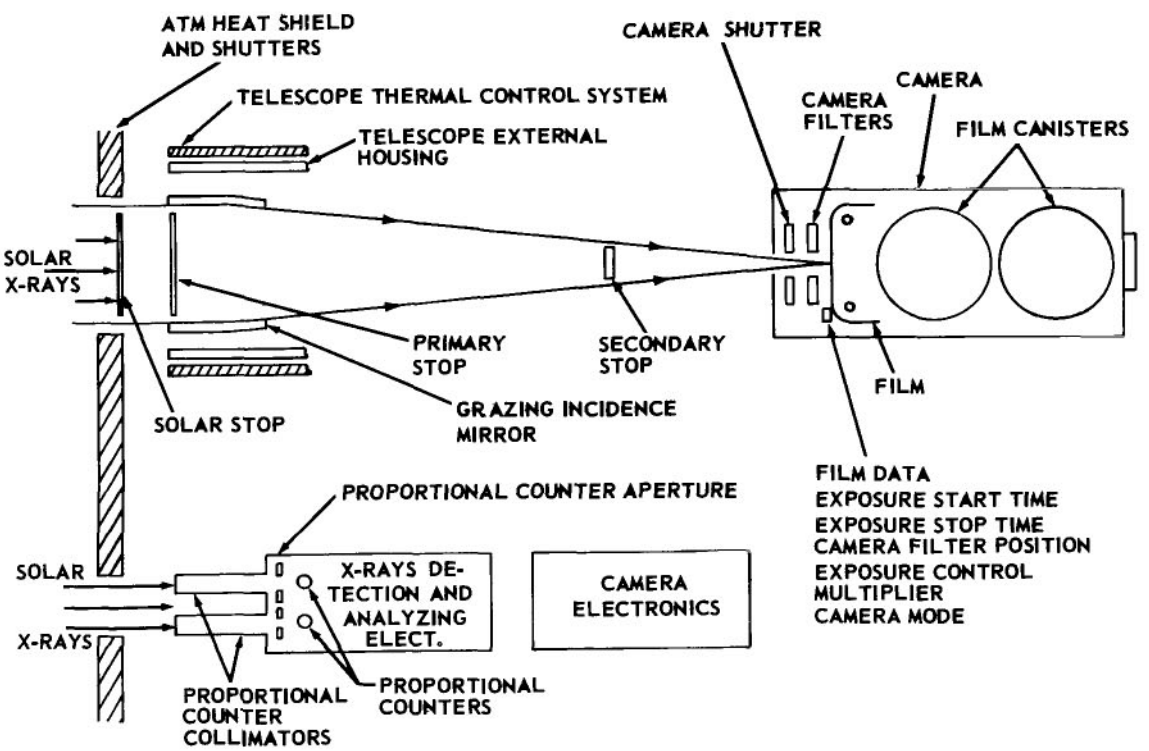

FIGURE 19. BLOCK DIAGRAM OF GSFC X-RAY TELESCOPE EXPERIMENT S 056

To measure the spectral distribution of transient solar events in the x-ray region, gas-filled proportional counters are used. Metallic windows on the counters provide a basic pass-band for x-ray photons, restricted by both a high- and a low-energy limit.

Proportional counters have the property of responding with output pulses which are linearly proportional to the energy of the detected photons. Analysis of the output pulses on an amplitude basis provides a satisfactory method of photon energy resolution. The process of sorting the pulses (in pulse-height analyzers) is performed with high speed digital circuitry, and therefore the speed of response of the proportional counters is not appreciably decreased.

Two limitations of proportional counters should also be identified. One is that the energy resolution is limited to no more than 15 percent ($\Delta E/E \gtrsim 0.15$). The other is that the characteristics of proportional counters change after a high but limited number (about one billion, 10^9) of photons have been detected.

Soft x-ray solar images are formed using a two-element, double-reflection aplanatic telescope (Fig. 20). Paraboloidal and hyperboloidal elements placed confocally to each other, and used in regions where their surfaces are nearly parallel to their axis of revolution, form surfaces that are at high angles of incidence to the incoming solar photons. The properties of such a combination are that incoming paraxial rays first strike the paraboloidal surface, undergo total external reflection, and are imaged toward the focal point. Before focusing, the rays strike the confocally placed hyperboloidal surface, where they again undergo total external reflection and are imaged at the hyperboloid's second focal point.

The camera's film plane is placed coincident with this second focal point and six different filters are positioned ahead of the film plane. The resulting data are solar filtergrams in the 5 to 60 Å region.

It is to be noted that the image quality of this focusing device is excellent on the optical axis, but is considerably degraded with small angular deviations from the optical axis.

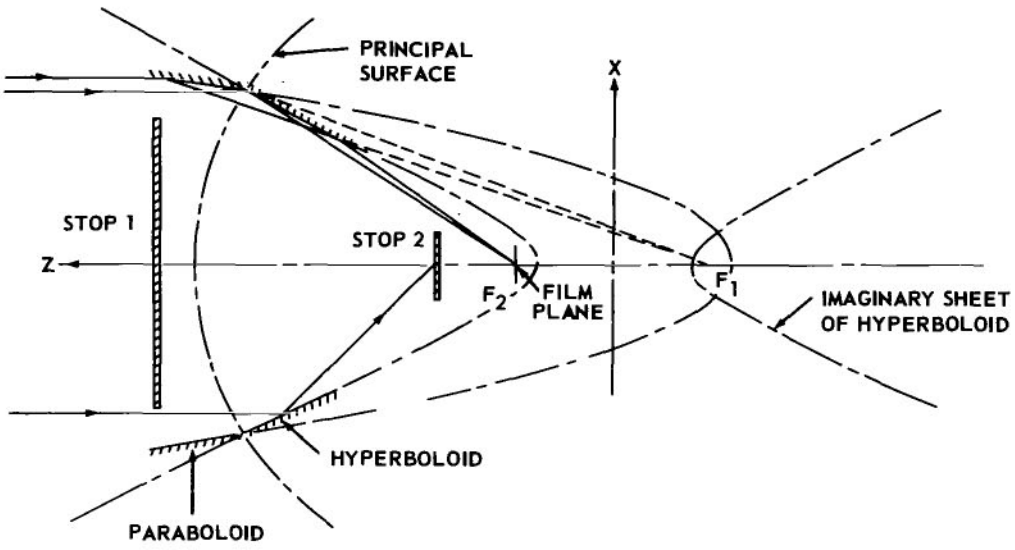

FIGURE 20. TWO-ELEMENT DOUBLE-REFLECTION APLANATIC TELESCOPE

ATM HYDROGEN-ALPHA TELESCOPE

By

Ed Miller

The prime function of the ATM hydrogen-alpha (H-α) telescope is to provide the astronaut with a television display of solar flare activity. The filter bandpass at the 6562.8 Å Fraunhofer H-α line is being chosen to optimize early flare recognition. The system also provides a backup to the Harvard College Observatory narrow bandpass H-α telescope.

The telescope (Fig. 21) is a 16.5 cm (6.5 in.) aperture, diffraction limited, f/30 Cassegrain with telecentric correctors and a vidicon television camera detector. A zoom relay lens allows fields of view over the range of 7 arc min to 35 arc min. With the 7 arc min field, the telescope has a resolution capability of 1.5 arc sec, allowing high resolution inspection of an active area for flare activity. With the 35 arc min field of view, the complete solar disk can be viewed for signs of flare activity. The telescope is boresight aligned to the ATM fine solar sensor to within ± 10 arc sec on the ground. After vehicle launch, this alignment will degrade to no more than one arc min.

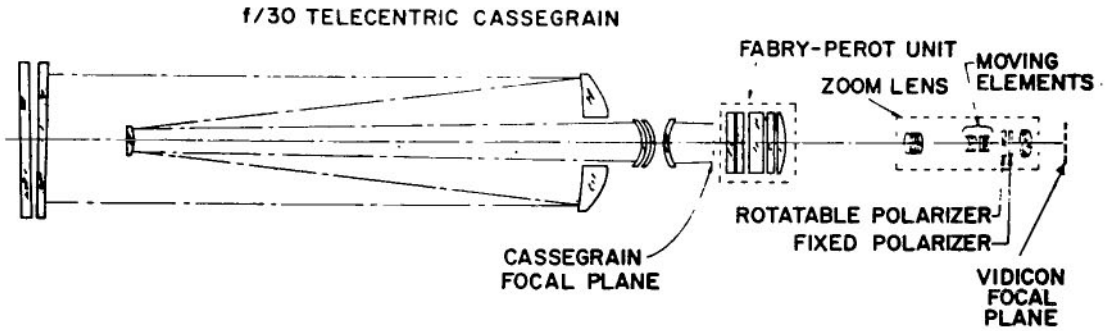

FIGURE 21. OPTICAL SCHEMATIC OF ATM HYDROGEN-ALPHA TELESCOPE

George C. Marshall Space Flight Center
National Aeronautics and Space Administration
Huntsville, Alabama, Oct. 1, 1968
948-89-00-0000-28-00-000

APPENDIX

TABLE A-I. ATM EXPERIMENT CAMERA AND FILM DATA

Experiment No. PI Vendor	Experiment Engineer	Camera Top Assembly Drawing	Unit Camera Materials and Dimensions (in.)	Unit Camera Weight (lb)	Return Camera or Magazine Quantity	Camera Pressurization & Quantity	Frames per Camera or Magazine	Film Type and Size	Maximum and Minimum Film Exposure	Film Wave Length (Å)	Radiation Limitation (Total Dosage)	ATM Data Encoded on Film
S 052 HAO BBRC	R. F. Harwell 877-2546	BBRC 25032 318-100-000	12 1/2 × 9 3/4 × 3 3/16 without handle (3½)	19.0 less handle (2 lb)	4 (cameras)	5.5 psia air 50% R.H. ± 10%	8025/cam. (32 100 total)	Pan X, 35 mm, 750 ft	1/2 sec to 4 1/2 sec	4000 to 7000 Polarized white visible light	10 rads d = 0.2 0.2 fogging density	Time, Roll
S 054 AS&E AS&E	T. W. Ponder 876-9696	481-000001 (Hycom)	25 × 17 × 8 includes handle plus appendages	37.0	4 (magazines)	± 2 psig (operating 2 psia)	5454/mag. (21 816 total)	unovercoated Pan X, 70 mm, 1000 ft	1/64 sec to 256 sec	2 to 60 X-ray	10 rads 0.2 density	Time
S 056 GSFC MSFC	H. D. Burke 876-8434	SK 2001	18 3/4 × 13 × 4 1/4 includes lens cover	12.5	4 (magazines)	zero psia (5 psia N_2 50% R.H. ± 10% in storage)	8000/mag. (32 000 total)	unovercoated Pan X, 35 mm, 1000 ft	1/3 sec to 320 sec	2 to 50 X-ray	10 rads 0.2 density	Multiplier, Time Open, Mode, Time Close, Filter
S 082B NRL BBRC	J. B. Franks 876-1655		16 1/2 × 16.18 × 6 1/4 21× 18 × 9 (box)	42.0 Mag. 15.0 Cam. 57.0 total	4 (magazines)	zero psia	1600/mag. (6400 total)	SWR, stripped, 20 × 250 mm	0.156 sec to 1200 sec	800 to 3000 Ultraviolet		Time, Roll Pitch, Yaw
S 082A NRL BBRC	J. B. Franks 876-1655		16 1/2 × 16.18 × 6 1/4 21× 18 × 9 (box)	42.0 Mag. 15.0 Cam. 57.0 total	4 (magazines)	zero psia	200/mag. (800 total)	SWR, stripped, 35 × 250 mm slides	0.156 sec to 1200 sec	170 to 650 Ultraviolet		Time
S 083 HCO MSFC	J. T. Power 876-7367	SK 4001	18 3/4 × 12 × 4 1/4 includes lens cover	12.5	2 (magazines)	5 psia N_2 50% R.H. ● 10%	16 000/mag. (32 000 total)	S0375, 35 mm, 1000 ft	1/100 sec to 1/25 sec	6562.808 ± 0.25 red visible light	20 rads 0.1 density	Time
H-Alpha #1 MSFC Perkin-Elmer	P. L. Hassler 876-3283	SK 3001	18 3/4 × 12 × 4 1/4 includes lens cover	12.5	4 (magazines)	5 psia N_2 50% R.H. ± 10%	16 000/mag. (64 000 total)	S0375, 35 mm, 1000 ft	1/100 sec to 1/25 sec	6562.808 ± 0.25 red visible light	20 rads 0.1 density	Time

TABLE A-II. ATM EXPERIMENT FILM DATA

Experiment No. PI Vendor	Film Storage				Removable or Auxiliary or Folding	Total Earth Return Vol. ($in.^3$)	Total Earth Return Weight (lb)	Field of View	Frame Angle From Z Axis	
	Ascent	Orbit (Prior to Use)	Orbit (After Use)	Descent						
S 052 HAO BBRC	Crew Provisions Module on Top of LM	MDA	MDA	CM	Removable handle	1560	76		0 degrees	
S 054 AS&E AS&E	Crew Provisions Module on Top of LM	MDA	MDA	CM	No folding or removable handle	9600 or if film can used the vol will be less than 1000	148		45 degrees	
S 056 GSFC MSFC	Crew Provisions Module on Top of LM	MDA	MDA	CM	Rem. handle, lens cover, 1 extra lens cover, seal-plate	$16 \times 4 \times 13$ 3500	50	40 arc min	60 degrees	
S 082A NRL BBRC	Crew Provisions Module on Top of LM	MDA	MDA	CM	Vacuum sealed box	13 608	228			
S 082B NRL BBRC	Crew Provisions Module on Top of LM	MDA	MDA	CM	Vacuum sealed box	13 608	228			
S 083 HCO AS&E	Crew Provisions Module on Top of LM	MDA	MDA	CM	Vacuum sealed box S 056	1750	25	18 arc min	0 degrees	
H-Alpha #1 MSFC Perkin-Elmer	Crew Provisions Module on Top of LM	MDA	MDA	CM	Vacuum sealed box	3500	50	35 arc min	0 degrees	
						47 126	805			Totals

NOTE: Both NRL A&B are stored and shipped in a hermetically sealed package under vacuum

TABLE A-III. ATM CAMERA/LM DISPLAY

Experiment	Experiment Data Camera	Slit Jaw Record	Sensor for LM Display	Type LM Display	Record of LM Display*
HAO S 052	Yes	No	Photo cells for internal and solar alignment	Null meter or scope	No requirement by PI
NRL "A" S 082A	Yes	No	None	None	N/A
NRL "B" S 082B	Yes	No	Vidicon camera of the slit	Outline of slit on solar disk	Desired by PI
NRL "XUV"	No	No	Vidicon camera of solar disk	XUV picture of the solar disk	Desired by PI**
AS&E S 054	Yes	No	Flare detector 48 × 48 sensor matrix on 1 arc min centers	CRT display of 48 × 48 arc min elements	Desired by PI
HCO "A" S 055A	No	No	Detector for Limb Crossing Meter (LCM)	LCM with white light signal. Data telemetered to ground.	No requirement by PI
HCO "B" S 055	Yes	Yes	Vidicon camera and detector for LCM	TV picture plus LCM with white light signal	No requirement by PI
HCO H-α #1 S 055A 0.5 Å Bandpass	Yes	No	Vidicon camera zoom 30 to 60 arc min	TV picture	No requirement by PI
GSFC S 056	Yes	No	Proportional counters used for flare indicators	Meter readout	No requirement by PI
MSFC H-α #2 2 Å Bandpass	No	No	Vidicon camera zoom 35 arc min to 7 arc min	TV picture	No requirement by PI

*Either a film or TV camera is being considered for permanent record of the LM display panel, decision pending.
**PI desires telemetering of some XUV pictures to ground.

[redacted]

PRELAUNCH ALIGNMENT REQUIREMENTS

		RACK PHY REF AXIS	SPAR PHY REF AXIS	CMG	ACQUIS. SS	ST	HAO	NRL-A	NRL-B	HCO-A	GSFC	AS & E	HCO H∞	ATM WL	FSS
RACK PHY REF AXIS	PITCH		±0°7'30"	±0°7'30"	±0°7'30"										
	YAW		±0°7'30"	±0°7'30"	±0°7'30"										
	ROLL		NONE	±0°7'30"	±¼°										
SPAR PHY REF AXIS	PITCH	±0°15'													±0°1'
	YAW	±0°15'													±0°1'
	ROLL	NONE													±0°1'
CMG	PITCH	±0°15'													
	YAW	±0°15'													
	ROLL	±0°15'													
ACQUIS. SS	PITCH	±0°15'				±0°0'30"									
	YAW	±0°15'				±0°0'30"									
	ROLL	±0°30'				±0°7'30"									
ST	PITCH				±0°1'				NONE	5					
	YAW				±0°1'				NONE						
	ROLL				±0°15'				±0°0'30"						
⊙ HAO	PITCH														±0°0'10"
	YAW														±0°0'10"
	ROLL														±0°30'
NRL-A	PITCH														±0°0'10"
	YAW														±0°0'10"
	ROLL														±0°30'
⊙ NRL-B	PITCH					NONE				±0°0'20"					±0°0'10"
	YAW					NONE				±0°0'20"					±0°0'10"
	ROLL					±0°1'				NONE					±0°15'
⊙ HCO-A	PITCH								±0°2'				±0°0'10"		
	YAW								±0°2'				±0°0'10"		
	ROLL								NONE				NONE		
GSFC	PITCH											±0°1'			±0°1'
	YAW											±0°1'			±0°1'
	ROLL											NONE			NONE
⊙ AS & E	PITCH										±0°2'				±0°1' *
	YAW										±0°2'				±0°1'
	ROLL										NONE				NONE
⊙ HCO H∞ (H∞1)	PITCH									±0°1'				±0°0'20"	±0°0'10"
	YAW									±0°1'				±0°0'20"	±0°0'10"
	ROLL									NONE				NONE	NONE
⊙ ATM WL (H∞2)	PITCH												±0°2'		±0°0'10"
	YAW												±0°2'		±0°0'10"
	ROLL												NONE		NONE
FSS	PITCH		±0°2'				±0°3'	±0°1'30"	±0°1'	±0°1'	±0°2'	±0°2'	±0°1'	±0°1'	
	YAW		±0°2'				±0°3'	±0°1'30"	±0°1'	±0°1'	±0°2'	±0°2'	±0°1'	±0°1'	
	ROLL		±0°2'				±1°	±1°	±0°30'	NONE	NONE	NONE	NONE	NONE	
POINTING ACCURACY REQMT	PITCH						±0°0'20"	±0°1'30"	±0°0'2½"	±0°0'10"	±0°2'	±0°1'	±0°1'	±0°1'	
	YAW						±0°0'20"	±0°1'30"	±0°0'2½"	±0°0'10"	±0°2'	±0°1'	±0°1'	±0°1'	
	ROLL						±5°	±5°	±0°10' △	NONE	NONE	±15°	NONE	NONE	
RATE GYROS	PITCH	±1° ROLL	NONE	±1° NONE											
	YAW	±1° GYRO	±1°												
	ROLL	NONE	±1°												

YAW GYRO

PITCH GYRO

ORBITAL ALIGNMENT REQUIREMENTS

LEGEND:

⊙ INTERNAL BORESIGHTING

ITE ROS	REMARKS
ROLL ROLL UE.	
±½° NONE ±½°	COALIGNMENT OF REDUNDANT RATE GYROS NOT REQUIRED
	YAW GYRO
	PITCH GYRO
	NULL ACCURACY OF ACQUISITION SUN SENSOR IS ± 2 ARC MINUTES IN PITCH & YAW
	NULL ACCURACY OF ST IS ± 30 ARC SECONDS FOR BOTH INNER & OUTER GIMBALS
	* SHIMS WILL BE USED TO MEET THE PITCH REQUIREMENT ONLY
	NULL ACCURACY OF FSS IS ± 1.7 ARC SECONDS IN PITCH & YAW
	△ THIS REQUIRES ZEROING THE EXPT. POINTING SYSTEM ROLL RESOLVER ZERO ORIENTATION TO NRL-B ZERO ROLL POSITION

REV E PRELAUNCH CONTINUED

15. FSS TO SPAR ±0°1' WAS ±0°2'
16. ACQUIS. SS TO FSS REMOVED PITCH & YAW WAS ±0°10'
17. REMOVED ST TO FSS PITCH & YAW WAS ±0°2'30" ROLL WAS ±0°1'30"
18. ADDED NRL-B TO HCO-C
19. HCO-C TO HCO H= PITCH & YAW ±0°0'25" WAS ±0°0'20"

ORBITAL

21. ADDED HCO-C TO NRL-B
22. ATM WL TO HCO H= PITCH & YAW ±0°2' WAS ±0°1'
23. AS & E TO HCO-C REMOVED PITCH & YAW WAS ±0°4'

REVISIONS

SYM	DESCRIPTION	DATE	APPROVAL
F	GENERAL REVISIONS	7-12-68	

1. HCO-A WAS HCO-C

REVISIONS TO PRELAUNCH ALIGNMENT REQ'MT

1. NRL-B TO HCO-A PITCH & YAW ±0°0'20" WAS ±0°0'5"
2. HCO-A TO HCO H= PITCH & YAW ±0°0'10" WAS ±0°0'25"

REVISIONS TO ORBITAL ALIGNMENT REQ'MT

1. HCO-A TO NRL-B PITCH & YAW ±0°2' WAS ±0°0'30"
2. HCO H= TO HCO-A PITCH & YAW ±0°1' WAS ±0°2'

REVISIONS

SYM	DESCRIPTION	DATE	APPROVAL
E		4-19-68	

REVISIONS TO PRELAUNCH ALIGNMENT REQ'MT

1. SPAR AXIS TO RACK AXIS PITCH & YAW ±0°7'30" WAS ±0°1'30", ROLL REMOVED WAS ±0°1'30"
2. CMG TO RACK AXIS ±0°7'30" WAS ±0°15'
3. CHANGED CSS TO ACQUIS. SS
4. ACQUIS. SS TO RACK PITCH & YAW ±0°7'30" WAS ±0°6', ROLL ±¼° WAS ±½°
5. ADDED ST TO ACQUIS. SS
6. ADDED NRL-B TO ST
7. REMOVED HCO-A & HCO-B
8. REMOVED AS&E TO NRL-B & HCO-C.
9. AS&E TO GSFC PITCH & YAW ±0°1' WAS ±0°2'
10. REMOVED HCO-C TO FSS
11. FSS TO NRL-B ROLL ±0°15' WAS 0°10'
12. REMOVED HCO H= TO AS & E
13. REMOVED ATM WL TO AS & E
14. AS & E TO FSS ROLL REMOVED WAS ±1°

REVISIONS TO ORBITAL ALIGNMENT REQ'MT

1. SPAR TO RACK PITCH ±0°15' WAS ±0°5' YAW ±0°15' WAS ±0°3' ROLL REMOVED WAS ±0°3'
2. CMG TO RACK AXIS ±0°15' WAS ±0°45'
3. ACQUIS. SS TO RACK PITCH & YAW ±0°15' WAS ±0°12', ROLL ±0°30' WAS ±1°
4. ADDED ST TO AQUIS. SS
5. ADDED NRL-B TO ST
6. REMOVED AS & E TO NRL-B
7. AS&E TO GSFC PITCH & YAW ±0°2' WAS ±0°4'
8. HCO H= TO AS & E REMOVED
9. REMOVED ATM WL TO AS & E
10. FSS TO SPAR ±0°2' WAS ±0°2'30"
11. REMOVED FSS TO ACQUIS. SS & ST
12. FSS TO NRL-B ROLL ±0°30' WAS ±0°15'
13. SUN CHANGED TO POINTING ACCURACY REQ'MT
14. POINTING ACCURACY REQ'MT TO ACQUIS. SS REMOVED
15. POINTING ACCURACY REQ'MT TO AS & E ROLL ±15° WAS ±2°
16. POINTING ACCURACY REQ'MT TO FSS REMOVED
17. FSS TO AS & E ROLL REMOVED WAS ±2°
18. CHANGES & ADDITIONS TO REMARKS
19. REMOVED NOTES 1 & 2, ADDED NOTE 5
20. ADDED "FOR ATM-A" TO TITLE BLOCK

10M03736 F

NOTES:

3. EXPERIMENTS WITHOUT ADJUSTABLE MOUNTING FEET (REF DWG 50M02426) MAY EXCEED THE PRELAUNCH ALIGNMENTS REQUIREMENT SHIMS ARE NOT CONSIDERED A MECHANICAL ADJUSTMENT.
4. MSFC WILL PERFORM ALIGNMENT BETWEEN OPTICAL (REFERENCE AXIS) TARGETS ONLY.
5. INITIAL ALIGNMENT WILL BE ±0°0'30". SUBSEQUENT VERIFICATION USING THE ROLL RESOLVER WILL BE ±0°7'30" WHICH INCLUDES ±0°1' INACCURACY OF THE ROLL RESOLVER & ±0°6' INACCURACY DUE TO GEAR TRAIN TOLERANCES. ALIGNMENT VERIFICATION SHOULD BE CHECKED EVERY 45° OF ROLL.

THIS DWG REPLACES SK10-7416

R-P&VE-VSL

ORIGINAL DATE OF DRAWING May 22, 67
DRAWN Benson
CHECKED D. Schrider
SUBMITTED W.P. Prosthofer
APPROVED ST R-P&VE-SS
PROJECTOR

APOLLO TELESCOPE MOUNT ALIGNMENT PARAMETERS FOR ATM-A

WEIGHT CHECKED | DATE | CODE
SCALE None | UNIT WEIGHT | SHEET 1 OF 1

GEORGE C. MARSHALL SPACE FLIGHT CENTER
NATIONAL AERONAUTICS AND SPACE ADMINISTRATION
HUNTSVILLE, ALABAMA

DWG SIZE D | 10M03786

NATIONAL AERONAUTICS AND SPACE ADMINISTRATION
WASHINGTON, D. C. 20546

OFFICIAL BUSINESS

FIRST CLASS MAIL

POSTAGE AND FEES PAID
NATIONAL AERONAUTICS AND
SPACE ADMINISTRATION

POSTMASTER: If Undeliverable (Section 158 Postal Manual) Do Not Return

"The aeronautical and space activities of the United States shall be conducted so as to contribute . . . to the expansion of human knowledge of phenomena in the atmosphere and space. The Administration shall provide for the widest practicable and appropriate dissemination of information concerning its activities and the results thereof."

—NATIONAL AERONAUTICS AND SPACE ACT OF 1958

NASA SCIENTIFIC AND TECHNICAL PUBLICATIONS

TECHNICAL REPORTS: Scientific and technical information considered important, complete, and a lasting contribution to existing knowledge.

TECHNICAL NOTES: Information less broad in scope but nevertheless of importance as a contribution to existing knowledge.

TECHNICAL MEMORANDUMS: Information receiving limited distribution because of preliminary data, security classification, or other reasons.

CONTRACTOR REPORTS: Scientific and technical information generated under a NASA contract or grant and considered an important contribution to existing knowledge.

TECHNICAL TRANSLATIONS: Information published in a foreign language considered to merit NASA distribution in English.

SPECIAL PUBLICATIONS: Information derived from or of value to NASA activities. Publications include conference proceedings, monographs, data compilations, handbooks, sourcebooks, and special bibliographies.

TECHNOLOGY UTILIZATION PUBLICATIONS: Information on technology used by NASA that may be of particular interest in commercial and other non-aerospace applications. Publications include Tech Briefs, Technology Utilization Reports and Notes, and Technology Surveys.

Details on the availability of these publications may be obtained from:

SCIENTIFIC AND TECHNICAL INFORMATION DIVISION

NATIONAL AERONAUTICS AND SPACE ADMINISTRATION

Washington, D.C. 20546